Biomacromolecules

pubs.acs.org/Biomac

Article

# Avidin-Conjugated Nanofibrillar Cellulose Hydrogel Functionalized with Biotinylated Fibronectin and Vitronectin Promotes 3D Culture of Fibroblasts

Jenni Leppiniemi,* Zeeshan Mutahir, Alexander Dulebo, Piia Mikkonen, Markus Nuopponen, Paula Turkki, and Vesa P. Hytönen*

Cite This: *Biomacromolecules* 2021, 22, 4122–4137

Read Online

ACCESS | Metrics & More | Article Recommendations | Supporting Information

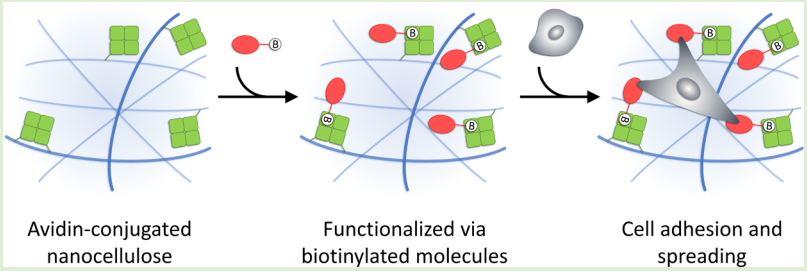


**ABSTRACT:** The future success of physiologically relevant three-dimensional (3D) cell/tissue models is dependent on the development of functional biomaterials, which can provide a well-defined 3D environment instructing cellular behavior. To establish a platform to produce tailored hydrogels, we conjugated avidin (Avd) to anionic nanofibrillar cellulose (aNFC) and demonstrated the use of the resulting Avd-NFC hydrogel for 3D cell culture, where Avd-NFC allows easy functionalization *via* biotinylated molecules. Avidin was successfully conjugated to nanocellulose and remained functional, as demonstrated by electrophoresis and titration with fluorescent biotin. Rheological analysis indicated that Avd-NFC retained shear-thinning and gel-forming properties. Topological characterization using AFM revealed the preserved fiber structure and confirmed the binding of biotinylated vitronectin (B-VN) on the fiber surface. The 3D cell culture experiments with mouse embryonic fibroblasts demonstrated the performance of Avd-NFC hydrogels functionalized with biotinylated fibronectin (B-FN) and B-VN. Cells cultured in Avd-NFC hydrogels functionalized with B-FN or B-VN formed matured integrin-mediated adhesions, indicated by phosphorylated focal adhesion kinase. We observed significantly higher cell proliferation rates when biotinylated proteins were bound to the Avd-NFC hydrogel compared to cells cultured in Avd-NFC alone, indicating the importance of the presence of adhesive sites for fibroblasts. The versatile Avd-NFC allows the easy functionalization of hydrogels with virtually any biotinylated molecule and may become widely utilized in 3D cell/tissue culture applications.

## 1. INTRODUCTION

In the natural milieu within all tissues and organs, majority of the cells are growing in a three-dimensional (3D) environment surrounded by the extracellular matrix (ECM). The ECM is mainly composed of water, proteins, and polysaccharides; however, each tissue has its unique ECM in terms of composition and topology, and ECM can serve as a reservoir for chemical factors important for the tissue, such as growth factors. The ECM not only provides an essential physical scaffolding for the cell constituents but also initiates crucial biochemical and biomechanical cues required for tissue morphogenesis, differentiation, and homeostasis.[1] Therefore, while 2D cultures are widely used, 3D cultures are needed to induce correct morphological and physiological responses, gene expression, cell polarity, and cellular morphology.[2] Nowadays, the cultivation of complex artificial tissues such as organoids, organs-on-a-chip, or 3D tissue models is in urgent need of suitable 3D cell culture methods.[3]

Hydrogels are flexible 3D polymer networks capable to retain a large amount of water in their swollen state.[4,5] Hydrogels are made of either natural or synthetic materials, and they may be cross-linked by covalent bonds or ionic complexation, via hydrogen bonding and via hydrophobic interactions.[4,6] Owing to their tunability, hydrogels have shown potential in several biomedical applications, including scaffolds for tissue engineering,[7] drug delivery,[8] contact lenses, wound

Received: May 6, 2021
Revised: August 25, 2021
Published: September 20, 2021

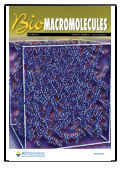





https://doi.org/10.1021/acs.biomac.1c00579
*Biomacromolecules* 2021, 22, 4122–4137

healing, and also in diagnostic devices.[9] As hydrogels mimic the natural ECM, they have been largely studied in 3D cell and organoid culture. In terms of 3D cell culture, the important parameters of hydrogels include mechanical strength, elasticity, porosity, ease of functionalization, biodegradability, and cell compatibility.[10,11]

A promising natural hydrogel material is nanofibrillar cellulose (NFC), also referred to as cellulose nanofiber (CNF). NFC can be extracted from wood or plants by a combination of mechanical, enzymatic, or chemical treatments.[12−15] NFC consists of cellulose nanofibers typically having a diameter ranging from 3 to 100 nm depending on the source and processing method, whereas the length is usually in the micrometer scale.[12,16] The surface of cellulose nanofibers is strongly hydrophilic due to a high amount of hydroxyl groups. Anionic cellulose nanofibers (aNFC) may be obtained, for example, by TEMPO (2,2,6,6-tetramethylpiperidine-1-oxyl)-mediated oxidization, which introduces negatively charged carboxyl groups on the surface of the fibers. This oxidization reaction also facilitates the disintegration of fibrils, leading to very thin fibers with a diameter of 3−4 nm.[17,18] NFC forms a hydrogel in water stabilized by weak interactions. However, the charged carboxyl groups of aNFC enable stabilization of the hydrogel or modification of the surface of nanofibers by ionic or covalent cross-linking chemistry.[15] Nanocellulose hydrogels are considered as biocompatible and bioinert materials to support cell growth and differentiation in a 3D environment even for several weeks, and they have shown promising results in numerous applications, including 3D cell and organoid culture, drug release studies, and 3D printing.[19−24] aNFC hydrogels have been shown to be cytocompatible with human adipose tissue-derived mesenchymal stem cells[25] and to support the cultivation of human embryonic stem cell-derived otic neuronal progenitor spheroids, while allowing sustained release of brain-derived neurotrophic factors from a polyhedron delivery system.[26]

The ability of hydrogels to serve as an optimal template facilitating cellular responses is a prerequisite for successful 3D cell culture. Excluding blood cells, most cells in our body are anchorage-dependent, which means that they must adhere to a substrate to survive. In the body, this substrate is often an ECM, a network of insoluble protein biopolymers, which can contain binding sites mediating interactions with cells. However, hydrogels intended for cell encapsulation are often lacking their own binding motifs, and therefore, adhesive motifs need to be incorporated into hydrogels to allow cell attachment and mediate cell viability.[27] For example, integrin-binding peptides such as Arg-Gly-Asp (RGD) can be conjugated into the hydrogel network to render it cell-adhesive.[28,29] Also, proteolytically cleavable peptides (such as GPQGIWGQ) have been incorporated into synthetic polyethylene glycol (PEG) hydrogels, allowing cell-mediated degradation by proteases such as matrix metalloproteases.[29]

In addition to directly conjugating adhesive peptides or proteins to the hydrogel network, an affinity interaction can be used to modulate hydrogels. Quite recently Barros et al. used affinity-based binding to incorporate laminin into synthetic PEG hydrogels. More specifically, a four-arm maleimide-terminated PEG macromer (PEG-4MAL) was functionalized with a mono-PEGylated recombinant human N-terminal agrin domain to promote high affinity binding of laminin. The authors showed that affinity-bound laminin PEG-4MAL hydrogels preserved laminin bioactivity better and enhanced human neural stem cell proliferation and neurite extension, when compared to hydrogels with physically entrapped laminin.[30] Another interesting affinity-based system is the interaction of avidin and biotin, which exploits the high specificity and extreme affinity ($K_d \sim 6 \times 10^{-16}$ M) of avidin toward biotin.[31−33] Avidin coating has already been used with polystyrene and biodegradable polymers such as poly(L-lactic acid (PLLA), poly(D,L-lactic acid (PDLLA), and polycaprolactone (PCL) to enhance adhesion of biotinylated chondrocytes, although the endocytosis of cell membrane-bound biotin molecules was reported to decrease the binding efficacy with time. To overcome endocytosis-related issues, the avidin−biotin system was used in combination with fibronectin (FN) to provide an integrin-dependent adhesion system. Indeed, enhanced cell adhesion and spreading of biotinylated chondrocytes were detected when avidin and FN solutions were co-adsorbed to PDLLA surfaces.[34] Similarly, the presence of FN has been shown to improve an *in vivo* osseous healing process in rabbits, when biotinylated fibronectin (B-FN) was incubated on biotin-streptavidin-coated titanium implant.[35] We previously used the avidin−biotin interaction for hydrogels, conjugating avidin to TEMPO-oxidized NFC and then combining the mixture with alginate and glycerol to obtain a suitable ink for 3D printing. Avidin retained its biotin-binding activity during the 3D printing process.[36] Also, avidin-conjugated gellan gum hydrogel has been prepared and functionalized by biotinylated adhesive ligands such as B-FN and biotinylated cyclic RGD; this was demonstrated to be a promising tool for 3D cell culture studies.[37] Recently, Fernandes et al. used avidin and biotinylated multi-arm PEGs to design affinity-triggered hydrogels. The authors showed that avidin and PEG-$[biotin]_4$ were capable to self-assemble instantaneously, and these hydrogels were used to encapsulate pluripotent stem cells and to induce neural lineage.[38]

In this *proof-of-concept* study, we conjugated avidin to aNFC and demonstrated that the avidin−biotin interaction could be used to functionalize the avidin-conjugated hydrogel with biotinylated proteins, providing cell adhesion motifs. We selected FN and vitronectin (VN) for chemical biotinylation as both serve as integrin ligands and contain an RGD-sequence. The performance of Avd-NFC hydrogel functionalized with B-FN or biotinylated vitronectin (B-VN) was demonstrated in 3D cell culture experiments. We observed a clearly enhanced cell viability and a more adhesive phenotype of mouse embryonic fibroblasts (MEFs), when cells were grown within Avd-NFC in the presence of the anchored biotinylated proteins compared to Avd-NFC or aNFC hydrogel alone. In principle, the Avd-NFC hydrogel allows functionalization virtually by any biotinylated molecule, including peptides, proteins, antibodies, growth factors, or other bioactive molecules promoting specific functions. Due to its wide tailoring capability, Avd-NFC may provide a valuable alternative to other commonly used and commercially available matrices, which support complex cell cultures, such as Matrigel.[39] Specifically, in contrast to Matrigel which is provided with varying concentrations of proteins and growth factors,[40] the Avd-NFC 3D culture setup can provide a platform to develop a tailored well-defined ECM for the growth of cells, spheroids, or organoids. These cultures can then be used for disease modeling, drug screening, or immuno-oncology applications.


https://doi.org/10.1021/acs.biomac.1c00579
Biomacromolecules 2021, 22, 4122−4137

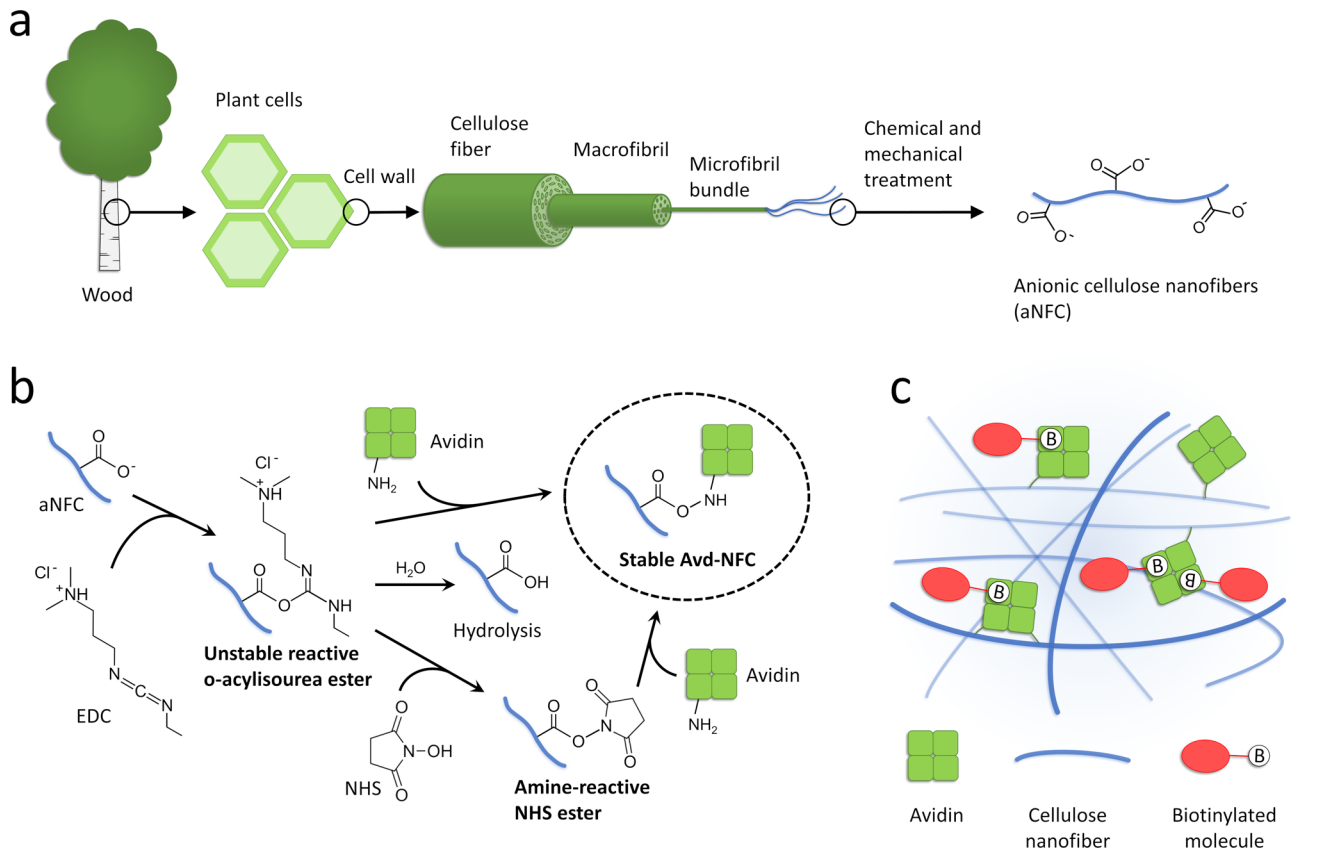


**Figure 1.** Production of avidin-conjugated nanocellulose. (a) Cellulose nanofibers can be produced from wood. Simplified schematic of the hierarchical structure of cellulose. (b) Reaction scheme for the covalent conjugation of carboxylic groups of anionic nanocellulose with amine groups of avidin using EDC/NHS-chemistry. (c) Schematic illustration of how the Avd-NFC matrix enables binding of biotinylated molecules. Figures are not shown in the correct scale.

## 2. EXPERIMENTAL SECTION

**2.1. Materials.** The aNFC hydrogel (GrowDex-T) and the commercially available avidin-conjugated nanofibrillar cellulose (Avd-NFC) hydrogel (GrowDex-A) were kindly provided by UPM Biomedicals, Finland. Recombinant charge-neutralized non-glycosylated chicken avidin (CNAvd) having a neutral isoelectric point (pI 6.93) was produced in*Escherichia coli*and purified by 2-iminobiotin affinity chromatography, as previously described.[41] *N*-Hydroxysuccinimide (NHS), 1-ethyl-3-(3-dimethylaminopropyl)carbodiimide hydrochloride (EDC), Pierce BCA protein assay kit, Ez-Link NHS-LC-biotin, HABA-dye (4′-hydroxyazobenzene-2-carboxylic acid), and low retention pipette tips were obtained from Thermo Fisher Scientific (Waltham, MA, USA). D-biotin was obtained from Fluka Chemie GmbH (Buchs, Switzerland), and the biotin (5-fluorescein) conjugate was purchased from Sigma-Aldrich (St. Louis, MO, USA). CellTiter-Glo 3D cell viability assay was acquired from Promega (Madison, WI, USA). Black polypropylene 96-well flat bottom plates were purchased from Greiner Bio-One (Kremsmünster, Austria). The cell culture media, high-glucose Dulbecco's modified Eagle medium (DMEM) supplemented with 1% (v/v) GlutaMax (Gibco), fetal bovine serum (FBS, Gibco), TrypLe Select (Gibco), and T75 cell culture flasks were obtained from Thermo Fisher Scientific (Waltham, MA, USA). Ultra-low attachment 96-well plates were obtained from Corning (Corning Life Sciences, Tewksbury, MA, USA), and 96-well glass bottom plates were obtained from Cellvis (Mountain View, CA, USA). Mini Protean TGX stain-free precast gels were purchased from Bio-Rad Laboratories (Hercules, CA, USA).

**2.2. Conjugation of Avidin to aNFC.** CNAvd was covalently conjugated via amine groups to carboxylic groups on NFC (Figure 1a) using EDC/NHS-chemistry using a protocol previously described.[36] All steps of the conjugation reaction were performed in a laminar flow hood, and ultrapure water was used to dissolve the reagents. Lyophilized, endotoxin-free CNAvd was dissolved in ultrapure water and sterile filtered (0.2 $\mu$m) to obtain a concentration of 1 mg/mL. aNFC hydrogel was used in its initial concentration of 1.0% (w/w). The principle of the conjugation chemistry is shown in Figure 1b.

Before conjugation, aNFC hydrogel was sonicated to homogenize the material and separate nanofibrils and aggregates, using a Sonics & Materials VC 505 sonicator with a 5 mm probe and a 25% amplitude. The samples were kept on an ice−water bath during sonication to prevent sample warming, and they were mixed during the sonication to obtain a homogeneous gel. The sonicated samples were mixed with an aqueous, sterile filtered (0.2 $\mu$m) suspension of EDC and NHS to achieve a concentration of 50 and 125 mM, respectively, and incubated at room temperature (RT, 21 ± 1 °C) for 15 min. The pH of EDC/NHS-activated aNFC was determined to be slightly acidic (pH ∼ 6). CNAvd protein (1 mg/mL) was added to the activated aNFC for covalent conjugation, using a ratio of 0.02 g of protein per 1 g of dry matter of nanocellulose. As a control sample, nanocellulose without EDC/NHS activation was used. The control samples were diluted with distilled water to the same extent as the activated nanocellulose before addition of avidin proteins. All reactions were first mixed well with a spatula and then incubated on a rolling shaker for 2 h at RT. Finally, the reactions were quenched by adding Tris−HCl (pH 8) to a final concentration of 20 mM. To remove non-conjugated avidin and non-reacted reagents, the conjugated product was washed twice by serially diluting the product in sterile water and centrifuging at 10,000*g* for 3 h at 20 °C. The supernatant was removed, and the hydrogel, now named Avd-NFC, was collected. The dry matter content of Avd-NFC was determined by comparing the wet weight of a sample to its dry weight after freeze-drying. The dry matter content was calculated by eq 1.



https://doi.org/10.1021/acs.biomac.1c00579
*Biomacromolecules* 2021, 22, 4122−4137

$$\text{Dry matter content (\%)} = \frac{\text{dry weight}}{\text{wet weight}} \times 100 \quad (1)$$

**2.3. Rheological Characterization of Hydrogels.** Rheological measurements were performed with a stress-controlled rotational AR-G2 rheometer (TA Instruments, UK) using plate geometry (diameter of plate 20 mm) at 22 °C. Two types of rheological tests were performed: flow profile measurements and shear stress amplitude sweep analyses. The flow profile was determined at different shear rates by gradually increasing the shear stress from 0.1 to 100 Pa. The yield point was determined as the intersection point between the linear region and viscosity drop region from the viscosity−shear stress plot. The shear stress amplitude sweep was measured with gradually increasing shear stress in the range of 0.01−100 Pa at the frequency of 0.1 Hz. Storage modulus ($G'$), loss modulus ($G''$), and yield stress were determined. Rheological experiments were performed for 0.5% (w/w) Avd-NFC, 0.5% (w/w) aNFC, and 0.5% (w/w) Avd-NFC functionalized with B-FN (50 $\mu$g/mL) or B-VN (50 $\mu$g/mL). Two parallel measurements were performed for each sample.

**2.4. Conjugation Efficiency of Avidin to Nanofibrillar Cellulose.** The conjugation efficiency of avidin to NFC was determined by gel electrophoresis mobility shift assay, comparing the Avd-NFC sample to a control sample (CNAvd + aNFC), where avidin was added to aNFC without any EDC/NHS reagent. In addition, bare CNAvd was analyzed as well. All samples were analyzed both in the absence and presence of D-biotin as biotin is known to stabilize the avidin tetramer. For this, samples were incubated for an hour at RT with a 10-fold molar excess of biotin, and samples without biotin were diluted with water to the same extent. A total of three parts of the sample were diluted with one part of 4 × SDS-PAGE sample-loading buffer containing 2-mercaptoethanol and heated to 50 °C for 20 min. Then, the samples were loaded to a Mini Protean TGX stain-free precast gel (Bio-Rad Laboratories, Hercules, CA, USA) in SDS-PAGE running buffer and run at 300 V for 15 min. This was followed by silver staining with a Pierce silver stain kit (Thermo Fisher Scientific, Waltham, MA, USA), and the gel was visualized with a ChemiDoc MP imaging system (Bio-Rad Laboratories) with Image Lab software. Theoretically, the amount of avidin loaded on the gel was 100 ng per sample, and the intensity of the bands on the gel was comparable to each other (Figure 3a). However, for the purified Avd-NFC, the amount of non-specifically bound protein removed from the sample during purification was not considered. The intensity of the protein band detected on the gel for Avd-NFC was compared to the control sample using ImageJ-software to determine the conjugation efficiency of avidin.

**2.5. Quantification of the Amount of Avidin in the Avd-NFC Hydrogel.** The amount of functional avidin in the purified Avd-NFC was determined to assess whether avidin remains functional and capable to bind biotin after conjugation to aNFC. A biotin (5-fluorescein) conjugate (B5F, Sigma-Aldrich) was used as it is brightly fluorescent free in solution, while the fluorescence is dramatically quenched when bound to avidin.[42] Purified Avd-NFC hydrogel was diluted to 0.2% (w/w) concentration in distilled water. A concentration series ranging from 0 to 4 $\mu$M of B5F was prepared in PBS, and the dilutions were added to a black 96-well plate (Greiner Bio-One). Then, Avd-NFC was added to each B5F dilution to obtain a 0.1% (w/w) final hydrogel concentration. Three parallel samples were measured for each B5F concentration. The samples were mixed well on a well-plate shaker, and the fluorescence of the samples was analyzed with a multilabel plate reader (Envision, Perkin Elmer) using a monochromator light path. When the fluorescence intensity is plotted versus the amount of B5F per sample, the intercept of non-linear and linear part determines the saturation point of avidin-binding sites, and thus, the concentration of available avidin can be determined. The amount of B5F [pmol] was plotted against the maximum emission intensity (Figure 3c). The performance of the assay was verified by incubating an Avd-NFC sample with a 10-fold molar excess of D-biotin prior to titrating with B5F. Also, aNFC was titrated with B5F as a control.

**2.6. Biotinylation of Fibronectin and Vitronectin.** Both FN and VN were purified from human plasma. For FN, gelatin affinity column chromatography was used, whereas VN was purified by heparin affinity chromatography.[43] Purified proteins were dialyzed in PBS (pH 7) and chemically biotinylated. An amine-reactive biotinylation reagent, Ez-Link NHS-LC-biotin (Thermo Fisher Scientific, MA, USA), was dissolved in DMSO to a 10 mM concentration. A 20-fold molar excess of this reagent was added to the FN solution and incubated for 30 min at RT. VN was biotinylated similarly, but a 30-fold molar excess of reagent was used. After biotinylation, proteins were dialyzed in PBS (pH 7) overnight to remove non-reacted biotin. The total protein concentration was determined with a Pierce BCA protein assay kit, and the number of conjugated biotins per protein molecule was determined according to the Pierce Biotin Quantitation Kit (Thermo Fisher Scientific), which is based on a colorimetric detection using HABA-dye and avidin.[44] The functionality of B-FN and B-VN was confirmed by coating standard cell culture-treated 96-well plates with the biotinylated proteins (10 $\mu$g/mL) or non-biotinylated FN and VN and comparing the growth of MEFs on both surfaces.

**2.7. Determination of the Availability of Avidin in the Avd-NFC Hydrogel for Biotinylated Molecules.** The available avidin-binding sites for larger biotinylated molecules were measured by indirect assay using B5F ($M_w$ 645 Da) and B-VN (~75 kDa). Samples containing Avd-NFC hydrogel 0.2% (w/w) and different amounts of B-VN were first mixed and incubated for an hour at RT. A concentration series ranging from 0 to 4 $\mu$M of B5F was prepared in PBS, and the dilutions were added to a black 96-well plate (Greiner Bio-One). Then, Avd-NFC + B-VN samples were added to each B5F dilution to obtain a 0.1% (w/w) final hydrogel concentration, and the samples were analyzed with a multilabel plate reader, as described in the quantification of the amount of avidin in the Avd-NFC hydrogel section. Two parallel samples were measured for each B-VN concentration. The determined values for available avidin were plotted against the amount of added B-VN, and as each B-VN contained 10.3 biotins per protein, the measured amount of available avidin was also plotted against the biotin content of the B-VN (Figure 3d).

**2.8. AFM Imaging.** Atomic force microscopy (AFM) was used for the characterization of cellulose nanofibers in aNFC, Avd-NFC, and Avd-NFC functionalized with B-VN. First, 0.1% (w/w) Avd-NFC was mixed with B-VN (final concentration, 0.05 mg/mL) and incubated at RT for 1 h. Prior to imaging, all hydrogel samples were diluted with water to 0.01% and sonicated for 5 min before spin-coating on freshly cleaved mica discs. Samples were imaged by a commercial BioScope Resolve AFM (Bruker Nano Inc, USA) in ambient air using the Peak Force QNM mode and ScanAsyst-Fluid probe. Images were analyzed using NanoScope Analysis software version 2.0 (Bruker Nano Inc., USA). The height profile was measured as a cross section of the fibrils on the sites where small spots (presumably protein) were seen on the fibril, and the height profile of the fibril alone was also measured. From height profile analysis, mean height ± standard deviation of plain fibrils or fibrils together with proteins was calculated.

**2.9. Cell Studies.** *2.9.1. Cell Culture.* The MEF cell line was a kind gift from Dr. Wolfgang Ziegler and has been previously described by Xu et al.[45] Cells were cultured in T75 flasks and maintained in high-glucose DMEM supplemented with 10% (v/v) FBS and 1% (v/v) GlutaMax (Gibco) in a humidified incubator at 37 °C and 5% $CO_2$. For 3D cell culture studies, fibroblasts were detached from the culture flask via enzyme (TrypLe Select, Gibco) treatment, then counted and diluted properly before embedding within hydrogels. The cells were regularly tested negative for mycoplasma contamination. MEFs between passages 10−17 were used for 3D cultivation in the hydrogels.

*2.9.2. Loading Biotinylated Proteins within the Avidin-Conjugated Nanofibrillar Cellulose Hydrogel.* Avidin-conjugated hydrogels [initial concentration 1.0% (w/w)] were first mixed with B-FN or B-VN and incubated for an hour at RT. As controls, non-biotinylated FN and VN were used. For biotin-saturated (negative) control, 19 $\mu$M D-biotin (meaning a 5-fold molar excess compared to the avidin


https://doi.org/10.1021/acs.biomac.1c00579
Biomacromolecules 2021, 22, 4122−4137

of Avd-NFC hydrogel) was added and incubated for an hour at RT with hydrogel. After incubation, the hydrogels were diluted with cell culture medium before addition of cells. In the final cell−hydrogel mixture, the concentration of NFC hydrogels (aNFC and Avd-NFC with and without biotinylated proteins) was 0.5% (w/v). The final concentration of biotinylated proteins, B-FN and B-VN, was 50 μg/mL. The final concentration of FBS (Gibco) was 10%.

*2.9.3. 3D Cell Culture in the Functionalized Hydrogel.* MEFs were embedded within Avd-NFC hydrogels functionalized with B-FN or B-VN to a seeding density of 100,000 cells/mL. Cell suspension was mixed with the hydrogel by pipetting gently up and down a couple of times until the mixture appeared visually homogeneous. Then, 100 μL of the cell−hydrogel mixture per well was added to 96-well plates [96-well glass bottom plate (Cellvis, CA, USA) for Live/Dead analysis and on ultra-low attachment 96-well plates (Corning, NY, USA) for CellTiter-Glo 3D cell viability assay]. After 30 min incubation at 37 °C, 100 μL of cell culture medium was gently added on top of the hydrogel. Samples were incubated at 37 °C and 5% $CO_2$. Every second or third day, the plates were centrifuged at 100 g for 5 min at RT, and half of the top layer medium was replaced with fresh cell culture medium.

*2.9.4. Cell Viability Assay.* Cell viability was determined by measuring the cytoplasmic ATP content of metabolically active cells using a CellTiter-Glo 3D cell viability assay (Promega, WI, USA) according to the manufacturer's instructions. The cell viability was determined on day 0, day 3, and day 7. The well plate was let to equilibrate to RT, then centrifuged at 200*g* for 5 min, and 100 μL of medium was removed from the well and replaced with 100 μL of CellTiter-Glo-reagent to lyse the cells. The plate was shaken for 5 min, centrifuged again at 200*g* for 5 min, and then incubated for 30 min at RT. The luminescence was recorded by a Envision multilabel plate reader (PerkinElmer, MA, USA). The mean of luminescence values measured for cell-free hydrogels was subtracted as a reference value. All samples were analyzed in triplicates, and the analysis was repeated at least in two parallel experiments. The relative luminescence units (RLUs) on day 3 and day 7 were normalized to the RLU measured on day 0.

*2.9.5. Live/Dead Staining.* Cell viability within hydrogels was determined by Live/Dead staining. For this, 100 μL of cell−hydrogel mixture per well was added on glass bottom 96-well plates (Cellvis, CA, USA), and then 100 μL of cell culture medium was carefully added on top of the hydrogel. The plate was Live/Dead stained after 3 days of cultivation. The plate was centrifuged at 100*g* for 5 min at RT, the medium of top of hydrogel was removed, and the samples were gently washed with PBS. The negative control sample was incubated with 1% saponin for 30 min, after which it was washed with PBS. Samples were stained with fluorescent dyes, Calcein AM (2.5 μM), and propidium iodide (2 μM), for live and dead cells, respectively. 100 μL of dye-PBS solution was added per well and incubated for an hour at 37 °C and 5% $CO_2$. As reference, the fibroblasts were grown on the well-plate (glass) bottom.

The stained samples were imaged using a Zeiss LSM 780 laser scanning confocal microscope (Carl Zeiss AG, Oberkochen, Germany) using a 25×/0.80, WD 0.57 mm objective and water as immersion medium. 488 nm and 561 nm lasers were used to excite Calcein AM and PI, and emission filters were from 493 to 582 nm for Calcein AM and from 582 to 718 nm for PI. Before imaging, the intensity of the lasers was adjusted according to the hydrogel sample containing highest number of live, fluorescent cells, and detector saturation was avoided strictly. In contrast, a control sample without any dyes produced insignificant background or autofluorescence. The imaging parameters were kept constant during a whole experiment to allow quantitative image analysis. For control samples such as cells only, Avd-NFC hydrogel with PBS only (no Calcein AM nor PI), and Avd-NFC hydrogel−cell mixture treated with 1% saponin, a thinner Z-stack (~100 μm with interval of 1 μm) was imaged, while for bioactivated hydrogels with cells, thicker Z-stacks (~300 μm with interval of 1 μm) were imaged to be able to observe the growth of cells inside the hydrogel. Images were taken using Zeiss Zen Black software and analyzed using ImageJ and Huygens Essential software. Maximum intensity projections of Z-stacks were prepared. For 3D views, a 3D viewer plugin was used with volume rendering option.

*2.9.6. Western Blot Analysis.* The cells cultivated within hydrogels were collected on day 3 and day 7 for Western blot analysis. The well plate was centrifuged at 100*g* for 5 min, and 100 μL of medium was removed from the top of the hydrogel. Then, 50 μL of 2 × Laemmli sample buffer containing 2-mercaptoethanol was mixed with hydrogel to lyse the cells. The plate was centrifuged again at 200*g* for 5 min, and the samples were collected in tubes. The cell lysates were boiled at 100 °C for 10 min and run on an SDS-PAGE to separate proteins. A wet blot system was used to transfer the separated proteins from gel onto a polyvinylidene fluoride membrane. The membranes were immunostained with antibodies against phosphorylated focal adhesion kinase (FAK pY397) (Abcam) and actin (Millipore). The details of antibodies are listed in Table S1. Primary antibodies were diluted in 5% BSA-TBS, 0.05% $NaN_3$, and 0.1% Tween 20 and incubated with membranes overnight at +4 °C with gentle shaking. The membranes were washed four times with TBS and 0.05% Tween 20. Appropriate secondary antibodies (LI-COR) were diluted in 5% BSA-TBS, 0.05% $NaN_3$, 0.1% Tween 20, and 0.01% SDS and incubated with blots for an hour at RT on a shaker. The membranes were washed four times with TBS and 0.05% Tween-20 and flushed once with TBS after which a LI-COR imaging system was used to detect the bound antibodies. The antibody intensities were analyzed using Image Studio Lite and ImageJ, and FAK pY397 values were divided by actin intensities. This Western blot analysis was repeated three times using parallel samples of two independent experiments. The ratio of intensity (FAK pY397/actin) of each sample was normalized against that of Avd-NFC to allow the comparison of parallel experiments.

*2.9.7. Statistical Analysis.* The statistical significance of differences was assessed by one-way analysis of variance (ANOVA) with Bonferroni's multiple comparison test in GraphPad Prism 5.02 software. $P < 0.05$ was considered statistically significant. In all figures, ns = not significant; * = $p < 0.05$; ** = $p < 0.01$; and *** = $p < 0.001$.

## 3. RESULTS AND DISCUSSION

**3.1. Avidin-Conjugated Nanofibrillar Cellulose Retains Its Hydrogel Properties.** After the covalent conjugation process of CNAvd and aNFC, the product was washed, and the dry matter content was determined. The obtained Avd-NFC formed a thick hydrogel, having a dry matter content of 2.2% (w/w) allowing handling with a spoon. For further studies, the product was mixed with sterile water and diluted to a dry matter content of 1.0% (w/w) to obtain a homogeneous product suitable for pipetting. Avd-NFC forms a transparent hydrogel, similar to the starting material aNFC.

The rheological properties of 0.5% (w/w) hydrogels were measured in the shear mode for all samples at a temperature of 22 °C. The viscosity of all samples decreased when higher shear rates were applied (Figure 2a), which is a typical behavior for shear-thinning materials. The viscosity of 0.5% (w/w) aNFC at low shear rates was ~3000 ± 900 Pa·s, whereas that for 0.5% (w/w) Avd-NFC was ~ 14,700 ± 2900 Pa·s. Therefore, conjugation of avidin to nanocellulose increased the viscosity of the Avd-NFC hydrogel at low shear rates. This may be due to the increase in the molecular weight of the polymers, but noncovalent interactions between avidin and nanocellulose may contribute as well. However, when the shear rate was increased, aNFC was found to be more elastic at higher shear rates before the final rupture of the gel. The yield point, which indicates the flow initiation at the level of applied stress, was 10.0 ± 0.0 Pa for aNFC, whereas that for Avd-NFC was lower, 1.4 ± 0.2 Pa.

All samples were also subjected to shear stress amplitude sweep analyses, and shear storage ($G'$) and loss ($G''$) moduli were measured as a function of shear stress (Figure 2b,c). In


https://doi.org/10.1021/acs.biomac.1c00579
Biomacromolecules 2021, 22, 4122−4137

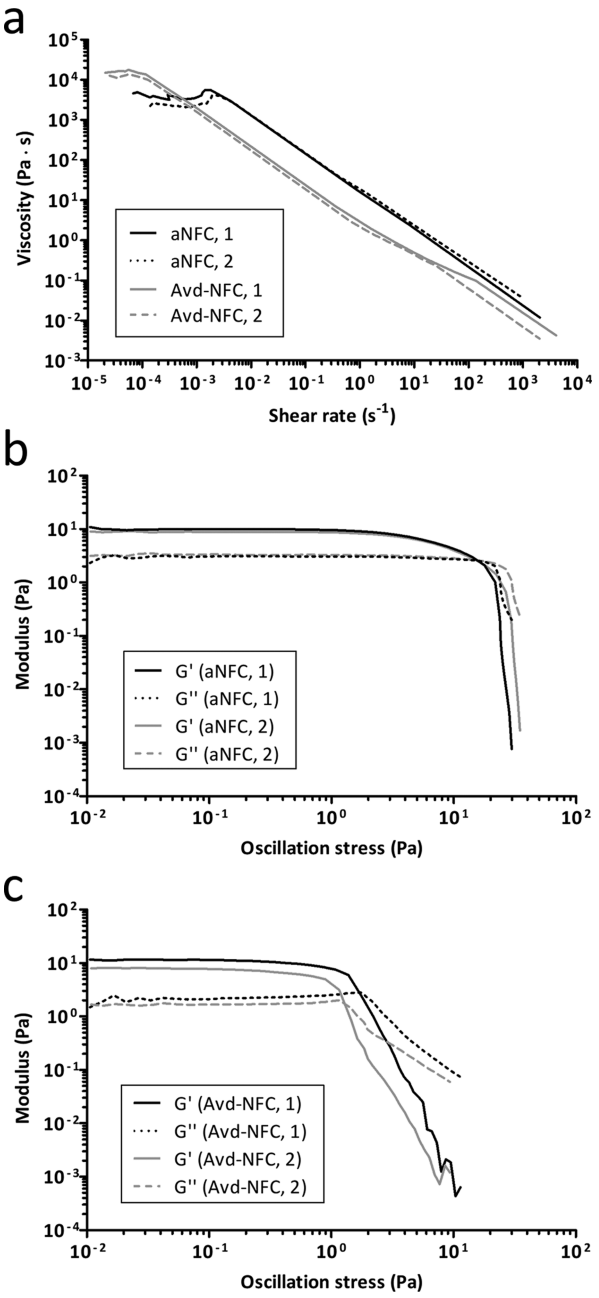


**Figure 2.** Characterization of aNFC and Avd-NFC hydrogels. (a) Viscosity as a function of the shear rate for aNFC and Avd-NFC. (b) Dynamic shear stress amplitude sweep analyses of aNFC and (c) Avd-NFC samples. Storage ($G'$) and loss modulus ($G''$) are shown as a function of the shear stress. Rheological characterization was performed for hydrogels at 0.5% (w/w) concentration, and the results for two parallel samples, 1 and 2, are shown.

the linear viscoelastic region (LVR), where the moduli are independent of the applied shear stress, $G'$ was higher than $G''$ for all samples, which indicates the elastic response to be stronger than the viscous one, which is typical for solid and gel-like structures. For aNFC, $G'$ was 9.4 ± 0.8 Pa and $G''$ was 3.2 ± 0.2 Pa, whereas for Avd-NFC, $G'$ was 9.5 ± 2.6 Pa and $G''$ was 1.9 ± 0.3 Pa. Outside the LVR, both the moduli started to decrease for both samples, indicating the breakdown of the gel structure. Surprisingly, the increase in the viscosity observed after conjugation of avidin (~3000 Pa·s for aNFC and 14,700 Pa·s for Avd-NFC) was not reflected in the storage modulus ($G'$), probably due to the disruption of the fibrillar network structure as a result of avidin conjugation.

We also studied how functionalization via biotinylated proteins affected Avd-NFC. While the changes were modest, we found that functionalization of Avd-NFC via B-FN decreased the storage modulus by 48%, as compared to Avd-NFC (Figure S1d,e). Functionalization of Avd-NFC with B-VN caused only minor change into storage modulus (increase by 10%) compared to Avd-NFC alone (Figure S1d,f). Since FN is a large protein with capability of forming fibrils while VN is a globular soluble protein, it is logical that FN conjugation leads to more significant changes in rheological properties of the hydrogel.

**3.2. Verification of Covalent Bonding of Avidin to aNFC.** The formation of covalent bonds between avidin (CNAvd) and aNFC was verified by SDS-PAGE mobility shift assay followed by silver staining. CNAvd is a tetrameric protein (size of tetramer ~56 kDa) containing several surface-exposed amine groups and may form one or several covalent bonds with the carboxyl groups of aNFC. When a covalent bond is formed between CNAvd and aNFC, the large molecular size of the Avd-NFC complex results in a very low mobility in the gel electrophoresis. Although being a tetramer, CNAvd may dissociate into monomers at elevated temperatures under reducing conditions, and in this case, monomers without covalent bond to aNFC are capable to penetrate the gel. Indeed, partial dissociation of CNAvd into monomers was detected on SDS-PAGE (Figure 3a) for Avd-NFC, control sample (CNAvd + aNFC), or bare CNAvd, which were heated to 50 °C for 20 min in the presence of 2-mercaptoethanol and SDS. However, incubating samples with a 10-fold molar excess of D-biotin before SDS-PAGE sample preparation stabilized the avidin tetramer,[46] and only tetramers were detected on the gel, as expected. For the Avd-NFC sample, analyzed in the presence of biotin, only a faint band of tetramers was detected on the gel, representing CNAvd tetramers with none of the four subunits covalently conjugated to aNFC. The conjugation efficiency of CNAvd tetramers was determined to be 86 ± 1% by comparing the intensities of the protein tetramer bands migrating into the gel from Avd-NFC [conjugated (1.), Figure 3a] and control sample (Figure 3a) in the presence of biotin. Avd-NFC samples were also analyzed on SDS-PAGE after purification. Purified and diluted [1.0% (w/w)] Avd-NFC samples were loaded on the gel in similar quantity (2.a, Figure 3a) or two-times lower amount (2.b, Figure 3a) compared to the conjugated Avd-NFC (1., Figure 3a). The amount of non-conjugated, soluble protein in the purified product appeared to be decreased after washing. However, the intensity of protein bands from the purified products is not directly comparable to those of control sample as the dry-matter content and gel composition changes during the purification process, while possible non-bound proteins and non-reacted reagents are being removed.

**3.3. Amount of Functional Avidin Present in the Avidin-Conjugated Nanofibrillar Cellulose Hydrogel.** The amount of functional CNAvd in Avd-NFC was determined by titration of small aliquots of B5F to diluted Avd-NFC. In the absence of avidin, the fluorescence of B5F was linearly dependent on its concentration, but when B5F bound to avidin, the fluorescence dramatically quenched and only a very small increase in fluorescence was detected after each titration (Figure 3b,c), as previously reported.[47] In fact, the early part of the titration curve shows a nonlinear response,


https://doi.org/10.1021/acs.biomac.1c00579
Biomacromolecules 2021, 22, 4122−4137

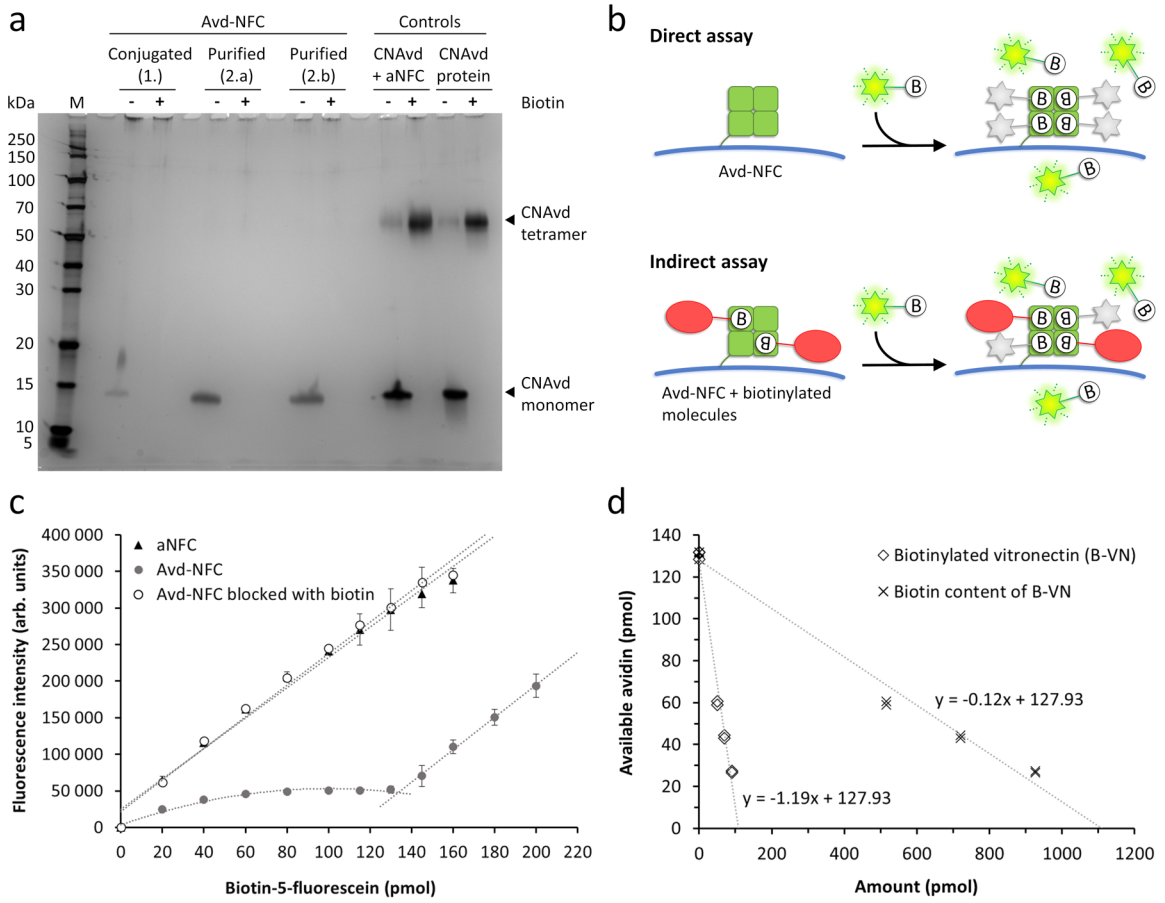


**Figure 3.** Determination of the biotin-binding capacity of the Avd-NFC. (a) SDS-PAGE analysis of covalent conjugation of CNAvd to aNFC. Covalently conjugated Avd-NFC samples were analyzed directly after conjugation (1.) and after purification (2.a and 2.b), together with a control sample in which CNAvd was mixed with aNFC without EDC/NHS activation (CNAvd + aNFC). Also, the CNAvd protein alone was analyzed in parallel. All samples were analyzed in the absence (−) and in the presence (+) of free D-biotin. Samples were heated at 50 °C for 20 min in the presence of 2-mercaptoethanol and analyzed by electrophoresis followed by silver staining. M is the molecular weight marker. (b) Schematic illustration of the principle of the biotin-5-fluorescein (B5F) binding assay to quantify the amount of active avidin in Avd-NFC samples. In the direct assay, Avd-NFC is titrated with B5F, whereas in the indirect assay, Avd-NFC is first loaded with biotinylated molecules and then titrated with B5F. Figures are not shown in the correct scale. (c) Quantification of the amount of active avidin (CNAvd) in Avd-NFC samples. Avd-NFC samples were diluted in distilled water and titrated with B5F. As a control, Avd-NFC was incubated with a 10-fold molar excess of D-biotin before titrating with B5F, and as a negative control, aNFC was titrated with B5F. Maximum fluorescent intensity is plotted vs. the amount of added B5F (pmol). The amount of active avidin is determined from the intersection of polynomial and linear trendlines. The measured values are shown as mean ± SD for three parallel samples. (d) Amount of available avidin for biotinylated conjugates was determined by indirect B5F assay using samples containing Avd-NFC and increasing amount of B-VN (50, 70, and 90 pmol). The measured data points are shown for two parallel analysis of each sample. As each B-VN contained 10.3 biotins per protein, the measured amount of available avidin is also plotted against the biotin content of the B-VN.

which most likely reflects the quenching arising from two factors: (1) the binding between B5F and avidin and (2) quenching due to B5F bound to adjacent binding site in tetrameric avidin.[48] After all biotin-binding sites being saturated with B5F, the fluorescence started to increase linearly (Figure 3c). When the fluorescence intensity was plotted against the amount of added B5F, the intersection of non-linear and linear part determined the saturation point of avidin-binding sites, and thus, the amount of functional avidin within each sample was determined. For control samples, aNFC and Avd-NFC incubated with 10-fold molar excess of D-biotin compared to ligand-binding sites of avidin, the fluorescence was linearly dependent on the concentration of B5F, suggesting the absence of nonspecific binding between B5F and NFC (Figure 3c). When the amount was calculated per known mass and volume of hydrogel, the result of functional avidin was 11.4 ± 0.2 $\mu$mol/L of hydrogel at 1.0% (w/w) concentration. The concentration of functional avidin can be expressed in another way as 0.16 mg/mL of Avd-NFC hydrogel at 1.0% (w/w) concentration, or 0.016 g or avidin per 1 g of dry matter of hydrogel. When considering the initial amount of avidin used in the conjugation reaction was 0.02 g or avidin per 1 g of dry matter of nanocellulose, we conclude that at least 80% of avidin become conjugated. However, during the protein expression, a small fraction of the binding sites of the avidin tetramer become saturated by endogenous biotin, and for avidin produced in *E. coli*, it has been shown that purified protein contained about 3.7 free biotin-binding sites per tetramer.[49] When taking this into consideration, we can estimate that the purified product contained ~0.017 g avidin per 1 g of dry matter of nanocellulose, and therefore, the estimated yield would be 85%. Overall, the conjugation reaction is efficient as the yield is between 80 and 85%, which is well in-line with the SDS-PAGE analysis results,


https://doi.org/10.1021/acs.biomac.1c00579
Biomacromolecules 2021, 22, 4122−4137

indicating 86 ± 1% coupling efficiency of CNAvd tetramers to nanocellulose.

**3.4. Avd-NFC Hydrogels Enable Biofunctionalization by Biotinylated Proteins.** *3.4.1. Biotinylation of Fibronectin and Vitronectin.* In order to functionalize Avd-NFC hydrogels for cell culture, we selected two proteins, FN and VN, which both have important roles in integrin-mediated cell adhesion. FN and VN were purified from human plasma and chemically biotinylated using amine-reactive biotinylation reagents, and the degree of biotinylation was determined using HABA-dye and CNAvd. The biotinylation reaction resulted in 12.5 mol of biotins per mole of FN and 10.3 mol of biotin per mole of VN. Both biotinylated proteins (B-FN and B-VN) were functionally active as standard cell culture surfaces coated with them supported the growth of MEFs similarly as the surfaces coated with non-biotinylated FN and VN controls (results not shown).

*3.4.2. Loading Capacity of the Avd-NFC Hydrogel for Biotinylated Proteins.* The avidin tetramer has four identical ligand-binding sites, which are arranged in a pairwise manner on opposite sides of the tetramer. D-biotin ($M_w$ 244.31 Da) and small biotin conjugates such as B5F ($M_w$ 645 Da) efficiently bind to the avidin tetramer in a non-cooperative manner. However, due to steric hindrance, larger biotin conjugates bind in an anti-cooperative manner, that is, the third and the fourth ligand associate more slowly and dissociate much faster than the first two ligands.[47,50] Consequently, we were interested whether all four biotin-binding sites of the avidin tetramer are available for larger biotinylated conjugates, when avidin is covalently conjugated to cellulose nanofibers as in Avd-NFC, as the attachment may cause steric hindrance for the binding. We quantified the available avidin-binding sites for larger biotinylated proteins by an indirect assay (Figure 3b) using B5F ($M_w$ 645 Da) and B-VN ($M_w$ ∼75 kDa), as described above. The amount of free avidin-binding sites decreased as the amount of added B-VN increased, as expected (Figure 3d). Using a linear trendline ($y = -1.19x + 127.93$) applied to the measured data points of added B-VN, we calculated that when $y = 0$, $x = 107.5$ pmol. This value represents the maximum binding capacity of 100 μL of 0.1% Avd-NFC hydrogel for B-VN, accounting also for the potential steric blockage of binding of B5F caused by B-VN. When considering that B-VN contained 10.3 mol of biotins per mole of VN, we plotted the amount of available avidin against the biotin content of the sample (Figure 3d). Again, we applied linear trendline ($y = -0.12x + 127.93$) to the data points and calculated that when $y = 0$, $x = 1066.1$ pmol. This is the theoretical maximum amount of biotins needed to saturate all available binding sites in Avd-NFC (0.1%). When the measured available CNAvd after addition of biotins of B-VN was normalized to the available CNAvd in Avd-NFC (0.1%), the results indicate that about 8.2 times molar excess of biotin compared of available avidin should be added to saturate all binding sites of Avd-NFC. However, full saturation may not be reached using large proteins. This is partially because the binding sites within the avidin tetramer are located as pairs, where two binding sites are in proximity. Populating both these two binding sites simultaneously with large biotinylated protein would be unlikely, and this phenomenon has been demonstrated previously with biotinylated PEG polymers: Ke et al. reported that the binding numbers of biotinylated PEG/avidin conjugates are highly dependent on the PEG chain length, which decreased from about four to one when the molecular weight of the PEG increased from 588 to 5000 Da.[51] Moreover, large particle, even flexible one, acts as entropic spring and therefore causes repulsion of the binding. Our results were well in line with previous findings of anti-cooperative binding of larger biotin conjugates to the avidin tetramer due to steric hindrance.[47] In summary, it is expected, that one avidin tetramer is not able to simultaneously bind four large biotinylated molecules, and this has to be taken into consideration when planning the experiments.

**3.5. Avd-NFC Preserved Fiber Structure Similar to aNFC.** When diluted (0.01%) aNFC and Avd-NFC samples were analyzed with AFM, the topography images (Figure 4a,b) revealed that both samples contained individual fibrils. In the case of Avd-NFC, some small bright spots were located here and there along the fibrils, presumably conjugated avidin proteins. Height profile analysis indicated that the mean height of the fibrils in aNFC was 2.5 ± 0.8 nm ($n = 6$). Similarly, in Avd-NFC, the mean height of plain fibrils was 2.5 ± 0.5 nm ($n = 6$), whereas the mean height of the fibrils in the presence of conjugated avidin was slightly increased to 3.0 ± 0.7 nm ($n = 6$). Thus, conjugated avidin only slightly increased the fiber height. The size of the avidin tetramer in solution has been determined by X-ray diffraction to be about 5 × 5 × 4 $nm^3$.[52] However, generally dry samples appear smaller (height and width) on AFM analysis compared to the native wet samples due to dehydration. Indeed, using AFM, Shao et al. reported that after drying with nitrogen gas, the height of the avidin tetramer was about 2.5−3 nm on the silicon surface,[53] and our findings are well in line with that. All samples showed some height variation within single fibrils, which may be attributed to intrinsic structure of the fibrils, such as twisting. However, we noticed that on the Avd-NFC sample, avidin protein was typically located on the side of the fibril rather than on top of it, and therefore, an increased fibril width rather than height was observed.

When Avd-NFC was functionalized with B-VN, even larger, very bright spots were clearly visible along Avd-NFC fibrils (Figure 4c). Here again, the mean height of plain fibrils was 1.9 ± 0.2 nm ($n = 8$), whereas that of the Avd-NFC fibrils with bound B-VN was notably higher, 5.1 ± 0.8 nm ($n = 8$). The size of the CNAvd tetramer is ∼56 kDa, whereas that of B-VN is ∼75 kDa. Based on the location of large spots along the fibrils and the resulting increment of fibril height, we assume that B-VN was bound to Avd-NFC fibrils via avidin−biotin interactions.

**3.6. Avd-NFC Hydrogels are Cytocompatible with MEFs.** Previously, NFC and aNFC hydrogels have been shown to be cytocompatible in several studies.[19,20,23,25,26] To assess the biocompatibility of Avd-NFC hydrogel, MEF cells were embedded within hydrogels to a seeding density of 100,000 cells/mL and cultured on ultra-low attachment 96-well plates with a layer of cell culture medium on top. The relative number of viable cells within samples was determined by CellTiter-Glo 3D cell viability assay at the beginning of the experiment (day 0) and after 3 or 7 days of culture. The original data of two independent experiments is shown in Figures S2a,b. The RLUs of three parallel samples on day 3 and day 7 were normalized by setting the luminescence values on day 0 to 1. The mean values of normalized samples are shown in Figure 5c. As low adhesion well plates do not support cell attachment, cells seeded directly on the plate could not adhere and eventually died during the assay. Therefore,


https://doi.org/10.1021/acs.biomac.1c00579
Biomacromolecules 2021, 22, 4122−4137

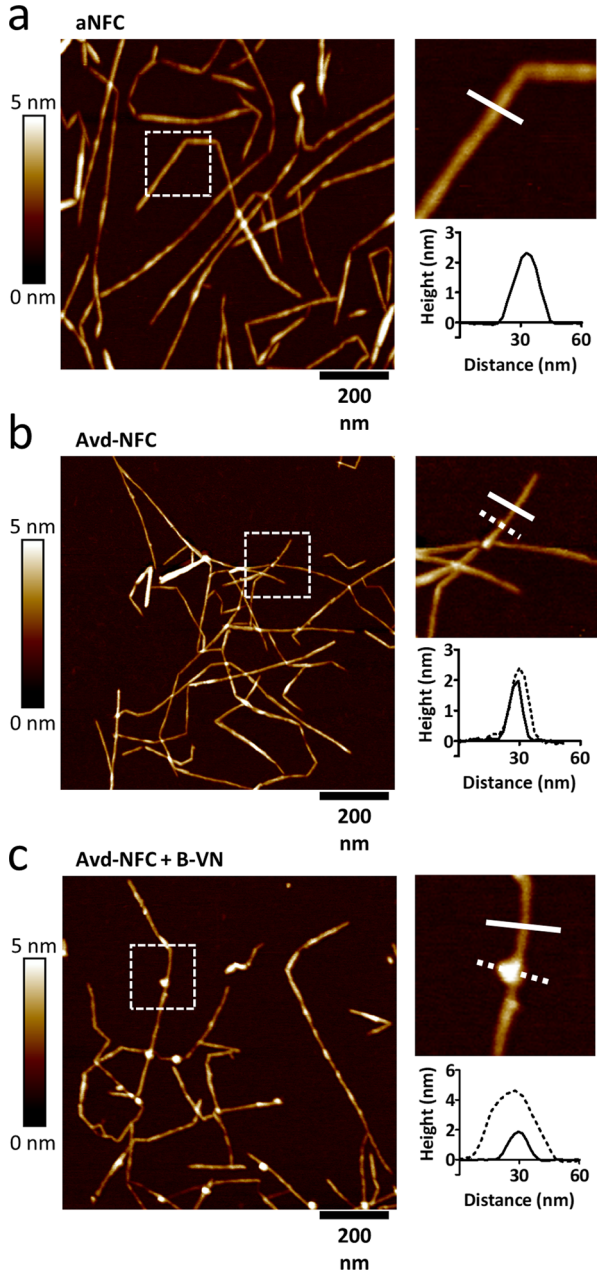


**Figure 4.** Topography of functionalized nanocellulose fibers. AFM analysis of cellulose nanofibers of (a) aNFC, (b) Avd-NFC, and (c) Avd-NFC functionalized with B-VN. AFM topography image (1 $\mu$m × 1 $\mu$m), magnified image (200 nm × 200 nm), and a height profile of fibrils corresponding to the lines in the magnified image are shown for each sample. A continuous line corresponds to the profile of a plain fibril, and a dotted line corresponds to the profile of a fibril together with a spot on it, where presumably avidin is conjugated to the fibril in (b), or where B-VN is bound to the Avd-NFC fibril (c).

samples containing cells but no hydrogel were used as a negative control for the assay.

The number of living cells increased within all hydrogels during the 7-day cultivation period, indicating that all the studied hydrogels were cytocompatible and provided suitable 3D matrix supporting cell proliferation (Figures 5c and S2). Significant differences were not seen between Avd-NFC and aNFC. Within Avd-NFC, the number of living cells increased 1.9 ± 0.2 times during 3 days and 6.6 ± 1.0 times during 7 days, whereas within aNFC, the number of living cells increased 2.4 ± 0.3 times during 3 days and 7.0 ± 0.6 times during 7 days ($p > 0.05$, $n = 6$ for each time point/sample). In this study, we used DMEM devoid of biotin; however, FBS contains biotin. As Avd-NFC is capable to bind biotin and this could have negative effect for cells, we tested whether the addition of 19 $\mu$M D-biotin (5-fold molar excess compared to avidin in the final hydrogel) to Avd-NFC before the addition of cells affected the cell viability on Avd-NFC. However, we observed no notable differences compared to Avd-NFC as the number of cells in Avd-NFC in the presence of biotin increased 2.0 ± 0.1 times after 3 days and further increased 8.2 ± 0.9 times after 7 days. Therefore, we concluded that the presence of avidin or its capability to harvest biotin from cell culture medium did not affect the growth of the fibroblasts, and Avd-NFC is equally well suited for fibroblast culturing as aNFC.

**3.7. Avd-NFC Hydrogel Functionalized with Biotinylated Adhesion Proteins Promotes Proliferation of Fibroblasts.** To study whether the availability of cell adhesion sites within a 3D hydrogel matrix had an effect on cell growth, we functionalized Avd-NFC with B-FN or B-VN before embedding cells. Nanocellulose hydrogels have been studied in different 3D cell culture applications, and depending on the cell type, the cell seeding densities varied between 10,000 and $9 \times 10^6$ cells/mL.[19,20,25] In our initial cell viability experiments, we used a cell seeding density of $1 \times 10^6$ cells/mL and noticed that the cell growth was especially high in the presence of B-VN. Therefore, we selected Avd-NFC functionalized with B-VN to test four different cell seeding densities; 100,000; 250,000; 500,000; and $1 \times 10^6$ cells/mL. We found out that cell viability was significantly increased in the lowest cell seeding density (Figure S3a,b), suggesting that with the higher cell densities, cells may suffer from lack of growth area or nutrients. For example, with a seeding density of $1 \times 10^6$/mL, the number of viable cells increased 2.9 ± 0.2-fold in 7 days, whereas with a seeding density of 100,000 cells/mL, the number of viable cells increased even 13.1 ± 0.7-fold in 7 days. Based on these results, we selected a cell seeding density of 100,000 cells/mL for further cell viability analysis.

With Avd-NFC functionalized with biotinylated adhesion proteins, we observed a notably higher cell growth during the test period than within Avd-NFC alone. In the presence of B-FN, the number of viable cells was 3.0 ± 0.5 times higher on day 3 and even 13.7 ± 3.4 times higher on day 7 compared to the initiation of the experiment on day 0 (Figure 5c). These values are significantly higher ($p < 0.05$, $n = 6$ on day 3; and $p < 0.001$, $n = 6$ on day 7) than those observed for Avd-NFC alone. In the presence of B-VN, the change was more dramatic as the number of viable cells increased 4.2 ± 0.8-fold in 3 days and 20.0 ± 4.5-fold in 7 days ($p < 0.001$, $n = 6$, when compared to Avd-NFC), showing that the presence of adhesion proteins can strongly promote cell proliferation. Both FN and VN provide RGD-cell attachment sites for adhesion-dependent cells. However, in order to physically mimic natural ECM and for the cells to experience the required mechanical cues, the adhesion molecules should be linked to the substrate. To evaluate whether the cell proliferation was due to increased cell adhesion, we used soluble, non-biotinylated FN and VN together with Avd-NFC to control the effect of the soluble adhesion molecules. In the presence of soluble FN, we observed a 2.4 ± 0.5 and 7.7 ± 1.3-fold increase in cell viability on day 3 and day 7, respectively. These values are much lower than those observed in the


https://doi.org/10.1021/acs.biomac.1c00579
Biomacromolecules 2021, 22, 4122−4137

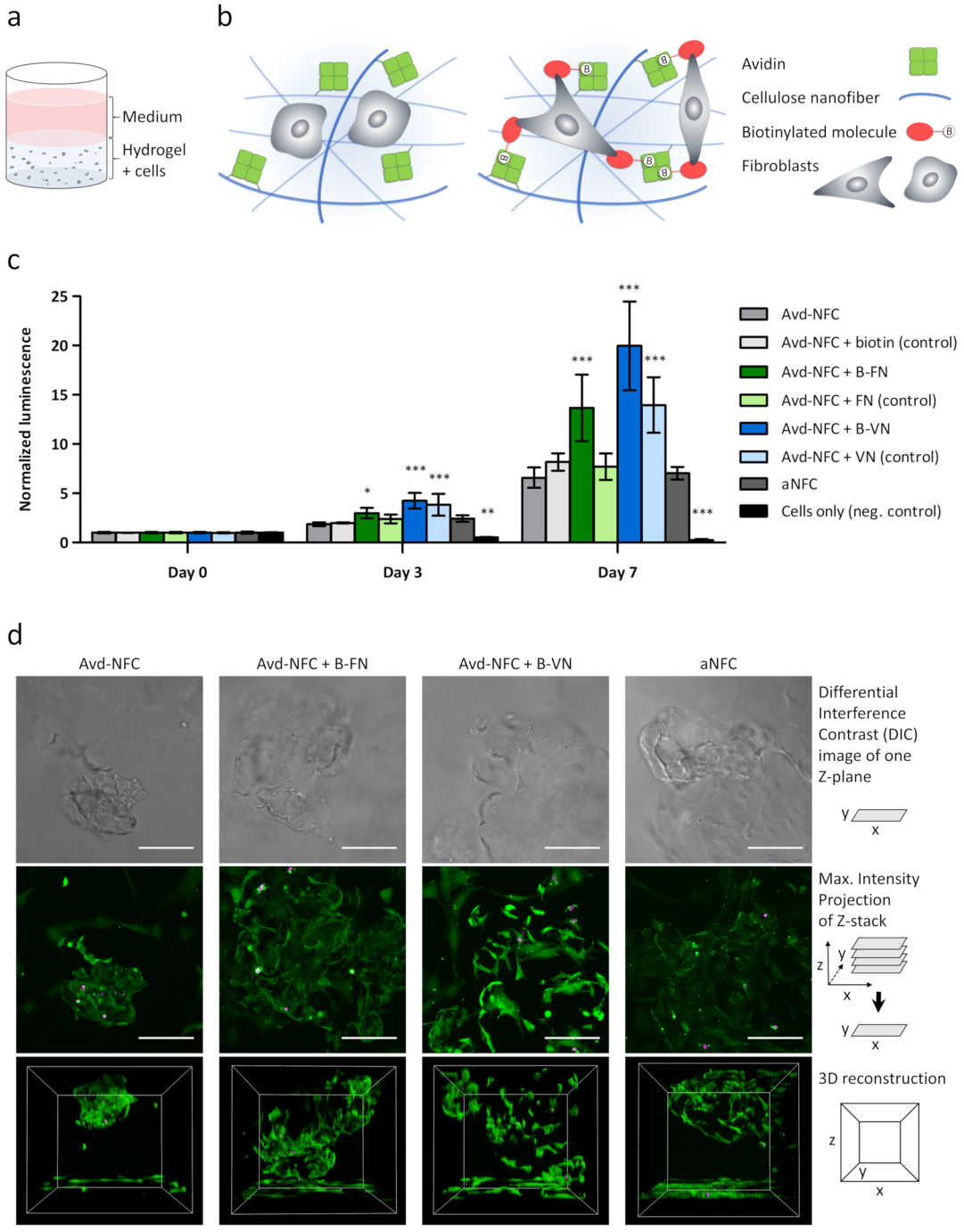


**Figure 5.** Culturing of fibroblasts in 3D hydrogels. When Avd-NFC hydrogels were functionalized with B-FN or B-VN, enhanced cell adhesion and spreading were detected. (a) MEFs were embedded within biofunctionalized hydrogels and applied onto a well plate. A layer of medium was added on top of the hydrogel. (b) Schematic of fibroblasts within different kinds of hydrogels. In the absence of adhesive cues, cells proliferate but do not find adhesion sites from Avd-NFC hydrogel, whereas biofunctionalized Avd-NFC hydrogel in the presence of biotinylated adhesion protein (B-FN or B-VN) provides adhesion sites for fibroblasts. (c) CellTiter-Glo 3D cell viability assay was used to determine the relative number of viable cells within different hydrogels. A cell seeding density of 100,000 cells/mL was used, and cell viability was determined on day 0 and after 3 and 7 days of cultivation. The RLU values on day 3 and day 7 of each sample were normalized by setting the luminescence values detected on day 0 to value 1. The bars are shown as mean ± SD for six parallel samples of two independent experiments, except Avd-NFC + biotin (control), for which the mean ± SD is calculated from three parallel samples of one experiment. Statistical analysis was performed by comparing to Avd-NFC using one-way ANOVA and Bonferroni's multiple comparison test, * = $p < 0.05$; ** = $p < 0.01$; and *** = $p < 0.001$. (d) Confocal microscopy imaging of MEFs within 0.5% (w/v) hydrogels stained with Calcein-AM (green, live cells) and propidium iodide (magenta, dead cells). Cells were embedded in different hydrogels (aNFC, Avd-NFC, Avd-NFC + B-FN, and Avd-NFC + B-VN) using a seeding density of 100,000 cells/mL and cultivated for 3 days. A differential interference contrast image of one Z-plane, a maximum intensity projection of Z-stack, and a 3D view are shown for each sample. The scale bars are 100 $\mu$m.



https://doi.org/10.1021/acs.biomac.1c00579
Biomacromolecules 2021, 22, 4122−4137

presence of B-FN. In fact, the cell viability in the presence of soluble FN does not significantly differ from Avd-NFC alone ($p > 0.05$, $n = 6$). Therefore, immobilization of B-FN to Avd-NFC was required for the enhancement of cell viability, further verifying that the effect was due to increased cell adhesion. For the soluble VN control, we observed a 3.8 ± 1.1 and 14.0 ± 2.8-fold increase in cell viability after 3 and 7 days, respectively, suggesting that even soluble VN can enhance cell viability ($p < 0.001$, $n = 6$, when compared to Avd-NFC alone). After 3 days of culture, the number of viable cells is very similar in the presence of B-VN or in the VN control. However, after 7 days, B-VN cells showed higher cell viability (20.0 ± 4.5) than the soluble VN control (14.0 ± 2.8).

In the course of this study, an Avd-NFC hydrogel produced by similar principles to our Avd-NFC became commercially available (GrowDex-A, UPM Biomedicals, Finland). We performed cell viability experiments and analyzed the effect of biotinylated adhesion proteins to the growth of MEFs within GrowDex-A as well. The results of a representative experiment are shown in Figure S4. The growth of cells within GrowDex-A had a similar trend to Avd-NFC hydrogels. Within plain GrowDex-A, the number of live cells increased 1.9 ± 0.2-fold on 3 days and 3.9 ± 0.4 times on 7 days. When GrowDex-A was functionalized with biotinylated adhesion proteins (B-FN and B-VN), the cell proliferation increased. After a 3-day cultivation, the increment in cell number was not yet statistically significant, but after 7 days, significant differences were observed. For example, in the presence of B-FN, the number of viable cells increased 2.2 ± 0.3-fold on 3 days and 6.7 ± 1.1-fold on 7 days ($p < 0.01$, $n = 3$, when compared to GrowDex-A). For GrowDex-A + FN (control), the number of live cells increased 1.8 ± 0.1-fold on 3 days and 3.8 ± 0.6-fold on 7 days, indicating the growth of cells to be very similar to GrowDex-A alone. Within GrowDex-A + B-VN, the cell proliferation was further increased; the number of live cells increased 2.5 ± 0.1-fold on 3 days and 9.2 ± 0.4-fold on 7 days ($p < 0.001$, $n = 3$, when compared to GrowDex-A). However, the proliferation of cells in the presence of VN seemed to be more or less independent of adhesion as a non-biotinylated VN control produced an effect similar to B-VN. This may reflect the differences between these integrin ligands. Adhesion on FN has been found to be dependent on the mechanical load, while VN appears to support integrin binding during early adhesion.[54] The results obtained with GrowDex-A further indicated that the adherence of cells to their surroundings supports their survival and proliferation in a 3D environment.

Substrate modulus may also influence on fibroblast behavior.[55] When cultured in a relatively soft environment ($E < 5$ kPa), fibroblasts are quiescent, while increased stiffness enhances cell proliferation and induces expression of $\alpha$-smooth muscle actin. Simultaneously, in 3D culture, increasing the hydrogel stiffness of covalently linked hydrogel may cause a negative effect on fibroblast proliferation.[56] When it comes to the current study, aNFC and Avd-NFC are weak hydrogels as they are not chemically or ionically cross-linked, and therefore, their stiffness is considered too low to induce fibroblast activation.

**3.8. Avd-NFC Hydrogels Functionalized with Biotinylated Proteins Enhanced Spreading of Fibroblasts into the Hydrogel.** Fluorescence staining and confocal imaging were used to visually study the distribution and morphology of the MEFs cultured within different NFC hydrogels, as shown in Figure 5d. In order to assess cytotoxicity, Live/Dead staining was used, and most cells were alive in all tested conditions, indicating that avidin conjugation to cellulose nanofibers was not harmful for the cells, and all studied hydrogels were cytocompatible. The control sample, cells only, is shown in Figure S5. The negative control sample, Avd-NFC treated with 1% saponin, showed high number of dead cells (results not shown). When Avd-NFC was functionalized with biotinylated proteins, B-FN and B-VN, cells were growing deeper inside the hydrogel, and the morphology was more elongated than with cells cultured in hydrogels without adhesion proteins. In the presence of B-FN and B-VN, cells also seemed to form more contacts with each other. Again, very similar findings were observed within GrowDex-A hydrogel as the number of live cells deeper inside the hydrogel seemed to increase when B-FN or B-VN was present (Figure S5). These results support our hypothesis that anchored FN and VN provide adhesion sites for MEFs and support their proliferation in 3D.

For 3D cell culture experiments, we chose to use the biotinylated proteins B-FN and B-VN in a final concentration of 50 $\mu$g/mL to measure their influence on cell growth and morphology within a 3D sample after extended culture. Both FN and VN are present in normal plasma at high concentrations (FN, ~300 $\mu$g/mL[57] and VN, 200−400 $\mu$g/mL[58]). As we used cell culture medium supplemented with 10% FBS, this alone does provide roughly a 20−40 $\mu$g/mL concentration of these proteins. Both FN and VN contain one RGD sequence. However, the proteins differ from each other in terms of their size as FN is a dimer consisting of ~220 kDa monomers, whereas VN has a molecular weight of ~75 kDa. Therefore, at a final concentration of 50 $\mu$g/mL, the molar concentration of RGD sequences provided by them was 0.23 $\mu$M in the case of B-FN and 0.67 $\mu$M in the case of B-VN (Table 1). As a result, at a 50 $\mu$g/mL concentration, B-VN provides 2.9 times higher molar amount of RGD-sequences than B-FN, which could partly explain the higher viability of MEFs in samples containing B-VN as the cells may find more adhesion sites in those hydrogels. However, the biotinylated proteins used have other differences as well. B-FN contained 12.5 biotins per monomer (~220 kDa), whereas B-VN contained 10.3 biotins per protein (75 kDa). Cellular FN may be assembled into an insoluble fibrillar network,[59] whereas VN is quite globular protein. Therefore, the distribution of the different sized and different kinds of biotinylated proteins may differ to some extent, which could reflect changes in cell viability as well. The final concentration of avidin (CNAvd) in

**Table 1. Concentration of Different Components of aNFC, Avd-NFC, and Avd-NFC Hydrogels Functionalized with B-FN or B-VN**

| | | concentration | | | |
|---|---|---|---|---|---|
| | | avidin | biotinylated protein | | |
| sample | dry matter content of hydrogel (%, w/v) | ($\mu$M) | (mg/mL) | ($\mu$M) | number of biotins per protein |
| aNFC | 0.5 | | | | |
| Avd-NFC | 0.5 | 5.7 | | | |
| Avd-NFC + B-FN | 0.5 | 5.7 | 0.050 | 0.23 | 12.5 |
| Avd-NFC + B-VN | 0.5 | 5.7 | 0.050 | 0.67 | 10.3 |


https://doi.org/10.1021/acs.biomac.1c00579
Biomacromolecules 2021, 22, 4122−4137

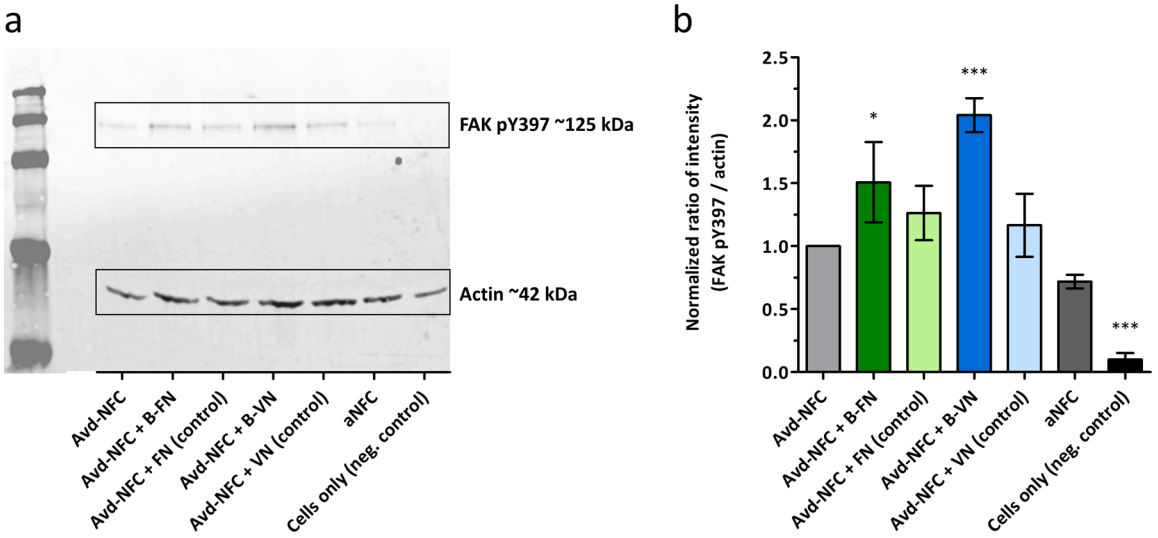


**Figure 6.** Analysis of FAK phosphorylation in 3D cell cultures. (a) Example of a Western blot used for quantification of FAK pTyr397. (b) Quantification of FAK pTyr397 levels from three parallel Western blots. For each sample, the ratio of intensity (FAK pTyr397/actin) was normalized against that of Avd-NFC. Bars represent mean ± standard deviation from three parallel analysis performed for samples collected after 7 days of cultivation. Statistical analysis was performed by comparing to Avd-NFC using one-way ANOVA and Bonferroni's multiple comparison test, * = $p < 0.05$; ** = $p < 0.01$; and *** = $p < 0.001$.

all our studied hydrogel samples [0.5% (w/w)] was 5.7 $\mu$M, whereas the concentration of biotin was 2.9 $\mu$M when hydrogel was functionalized with B-FN (50 $\mu$g/mL) or 6.9 $\mu$M when functionalized with B-VN (50 $\mu$g/mL). Although the total concentration of biotin in the B-VN sample was a bit higher than the amount of avidin, we are convinced that B-VN was efficiently bound because each VN contained ~10 biotins.

Previously, Broguiere et al. studied cultivation of epithelial organoids in fibrin matrices. Based on the physical properties of the studied hydrogels, they selected a fibrin concentration of 3 mg/mL and found that fibrin gel supplemented with 10% Matrigel had a similar colony formation efficiency than pure Matrigel, whereas the efficiency of the fibrin matrix alone was significantly lower. Interestingly, 3 mg/mL fibrin gel provided ~35 $\mu$M RGD sites, whereas Matrigel supplement (10%) provided only additional 0.7 $\mu$M RGD sites. The authors further analyzed fibrin matrices supplemented with different ECM components and identified that laminin-111 was the main ECM component needed for colony formation as 3 mg/mL fibrin matrix with 0.5 mg/mL laminin supplement led to stem cell proliferation and formation of rounded cysts, while a further increase in the laminin supplement to a concentration of 2 mg/mL (corresponding to ~2.2 $\mu$M concentration) produced results comparable to pure Matrigel.[60] Also in hydrogels, the concentration of immobilized RGD peptides has been studied. Enemchukwy et al. cultivated epithelial cells within RGD-conjugated PEG-4MAL hydrogels and found that during a 2-day cultivation, cell proliferation was insensitive to the RGD concentration (0−2 mM), whereas at least 2 mM concentration was needed to support the cyst formation in 10 days within hydrogels.[61] Recently, Curvello et al. cultivated small intestinal organoids within nanocellulose hydrogels conjugated with RGD peptide (2 mM) and further mixed with glycine. They found that RGD did not influence overall cell viability but was needed to support organoid development and bud formation.[62] In our studies, we observed a remarkable increase in the proliferation of MEFs in Avd-NFC hydrogel in the presence of B-FN and B-VN at a concentration of 50 $\mu$g/mL, corresponding to a RGD concentration of only 0.23 or 0.67 $\mu$M, respectively.

In addition to the importance of the RGD concentration, also the conformation of the RGD peptide affects the binding of cells. For example, Wacker et al. cultivated epithelial cells on RGD peptide-containing PEG hydrogels and found that cells showed higher initial adhesion strength on cyclic RGD, whereas linear RGD peptide produced increased focal adhesion formation and better long-term adhesion in flow.[63] Kumagai et al. again investigated mouse B16 melanoma cells on FN-coated wells and found that cyclic RGD inhibited cell attachment at a 20-fold lower concentration than the linear form.[64] Kapp et al. performed a systematic comparison by ELISA-like solid phase binding assay and measured the binding affinity of a wide range of RGD ligands to the RGD-binding integrins $\alpha v\beta 3$, $\alpha v\beta 5$, $\alpha v\beta 6$, $\alpha v\beta 8$, $\alpha 5\beta 1$, and $\alpha$IIb$\beta 3$. Their work showed that the binding affinity for these ligands strongly varied among different integrins.[65] These studies and our results suggest that both concentration and conformation of cell adhesion motifs within hydrogels may be largely cell type- and application-dependent, and therefore, further studies are required. The Avd-NFC material presented here offers an attractive platform to build suitable environments for various needs by only changing the biotinylated compounds.

**3.9. Fibroblasts Cultivated within Hydrogels in the Presence of Anchored Adhesion Proteins Showed Increased Adhesion.** Cell adhesion to the surrounding matrix is a very complex process, where integrins play a central role. Integrin-mediated cell adhesion regulates several dynamic cellular processes such as cell migration, phagocytosis, growth, and development.[66] Integrins are large transmembrane proteins, which consist of $\alpha$- and $\beta$-subunits assembling into heterodimers.[67] In their active state, the extracellular part binds to proteins of the ECM or proteins on other cells, whereas the intracellular part is connected to the actin cytoskeleton via several adapter and signaling proteins. In vertebrates, 18 $\alpha$ and 8 $\beta$-subunits can assemble into 24 different receptors with


https://doi.org/10.1021/acs.biomac.1c00579
Biomacromolecules 2021, 22, 4122−4137

different binding properties.[67] For example, αVβ3 integrin can bind to multiple ECM proteins including VN and FN.[54]

As discussed above, the presence of B-FN within Avd-NFC hydrogels increased cell proliferation ~13.7 ± 3.4-fold in cell viability assays, whereas soluble FN could increase cell proliferation only ~7.7 ± 1.3-fold, quite similar to Avd-NFC alone (6.6 ± 1.0-fold), suggesting that the increase in cell growth was due to better adhesive properties of the hydrogel. However, the presence of B-VN increased cell proliferation ~20.0 ± 4.5-fold, whereas also soluble VN increased cell proliferation ~14.0 ± 2.8-fold, suggesting that cells can take advantage of FN and VN differentially. Indeed, it has been shown that αVβ3 integrin binding to FN is force-dependent and would thus require anchoring of FN, whereas VN binding happens already under low-force conditions and may be adhesion-independent.[54]

To analyze the cell adhesion in more detail, we collected samples of cells cultured within different hydrogels after 3 or 7 days and performed Western blot analysis and immunolabeling against a cell adhesion marker, FAK pY397. If force-dependent adhesion maturation takes place, we should see an increase in the phosphorylation status of FAK at Y397. A representative Western blot is shown in Figure 6a, and blots from replicate experiments are shown in Figure S6a,b. We analyzed the ratio of intensity of FAK pY397 versus actin in the samples and normalized them against Avd-NFC (Figure 6b). This ratio was ~1.5 ± 0.3-fold higher ($p < 0.05$, $n = 3$) in Avd-NFC + B-FN compared to plain Avd-NFC, whereas in Avd-NFC + FN (control), the ratio was about 1.2 ± 0.3 times higher ($p > 0.05$, $n = 3$) than that in Avd-NFC. In Avd-NFC + B-VN, the ratio of FAK pY397 versus actin was even 2.0 ± 0.1 times higher ($p < 0.001$, $n = 3$) compared to Avd-NFC, while it was ~1.2 ± 0.3 times higher ($p > 0.05$, $n = 3$) for Avd-NFC + VN (control) compared to plain Avd-NFC. Thus, FAK pY397 was elevated in the presence of the biotinylated adhesion proteins, B-FN and B-VN, indicating that cells were able to attach to the anchored adhesion molecules and thus receive correct mechanical signals, whereas soluble VN and FN controls both showed lower levels of FAK pY397, similar to Avd-NFC alone. As the samples were cultivated on low adhesion well plates where cells were not able to attach, cells alone showed significantly lower level of FAK pY397 compared to samples where cells were embedded in hydrogels.

**3.10. Potential Applications of Avd-NFC in 3D Cell and Tissue Culture.** The natural ECM is a network of insoluble proteins and biopolymers, which contains binding sites mediating interactions with cells as most cells require adhesion to substrates for survival and correct function. The recent progress in 3D spheroid and organoid culture has been largely based on the use of biological basement membrane extracts such as Matrigel or similar products to support three-dimensional cell growth. Because of the animal-derived origin, the exact composition of the biological matrices is not always known, and they can have batch-to-batch variations, which may pose reproducibility problems in research.[68] Therefore, several natural and synthetic hydrogels have been studied as alternatives. However, as most hydrogels lack cell adhesion motifs, those need to be incorporated into hydrogels to allow cell attachment and mediate cell viability.[27]

The avidin−biotin interaction in hydrogel biofunctionalization offers the advantage of flexibility as Avd-NFC allows the straightforward and easy functionalization of hydrogel with different biotinylated molecules. As each tissue has its unique composition of ECM,[1] various 3D cell/tissue culture applications may require numerous different cues to be studied. With Avd-NFC, it would be even possible to study a mixture of different biotinylated ligands, which would however require careful optimization. Moreover, while the incorporation cell adhesion motifs into the hydrogel matrix is clearly important in modulating cell attachment, the spacing of cell adhesion motifs may also be important. For example, on 2D surfaces, cells are known to be highly sensitive to interligand spacing, which may alter cell morphology or differentiation.[27] In line with this are observations that 3D cell culture within PEG hydrogels modified with RGD motifs do not support cellular interactions below a certain RGD concentration.[29] However, the role of precise ligand spacing in 3D networks has been explored only recently.[27] In addition, the spacing may depend on the ligand used. For example, when using RGD peptides for hydrogel functionalization, higher molar concentration may be needed compared to the FN or VN used in this study. One of the advantages of Avd-NFC is that the concentration of biotinylated molecules, that is adhesive motifs, may be easily adjusted and studied in more detail according to the specific needs. Moreover, there are numerous biotinylated chemicals and proteins readily available in the market, and a vast amount of biotinylation tools available for the preparation of novel biotinylated molecules.[69] Biotin is a chemically inert, non-toxic, and rather stable molecule, which can be covalently attached to various biomolecules with high efficiency using mild chemical reaction condition. Also, site-specific biotinylation can be achieved posttranslationally using a biotinylation tag (AviTag).[70,71] In addition to proteins and small molecules, also whole cells can be biotinylated and could be directly applied on Avd-NFC. For example, biotinylated chondrocytes have been studied on avidin-coated polystyrene, PLLA, PDLLA, and PCL surfaces.[34]

The avidin−biotin interaction is based on extremely high affinity and specificity, which guarantees that biotinylated proteins can be very efficiently bound to the Avd-NFC hydrogel. We compared the results obtained with Avd-NFC functionalized with B-FN and B-VN to controls where FN and VN were simply mixed with Avd-NFC. Although in the control samples, the adhesion proteins may also be simply adsorbed or physisorbed to Avd-NFC, most likely the physisorption is not very efficient, and at least some portion of the protein will stay freely floating within the hydrogel. Indeed, FN-mediated adhesions are known to be mechanically active as the cells need to pull on the molecule and sense the ECM via this interaction, and here, we were unable to reproduce the effect that B-FN had on cell proliferation simply by mixing soluble FN with the hydrogel. Our results of cell viability studies demonstrated that fibroblasts were proliferating more efficiently in Avd-NFC and GrowDex-A hydrogels in the presence of B-FN or B-VN, when compared to their non-biotinylated controls, FN or VN. In addition, there was a marked increase in the adhesion maturation marker FAK pY397 in cells cultivated within Avd-NFC + B-FN or especially within Avd-NFC + B-VN compared to control samples containing Avd-NFC and non-biotinylated FN or VN (Figure 6). Especially, the specificity and efficacy of affinity-based avidin−biotin interaction make it a cost-efficient approach, as the used bioactive agent is efficiently bound to Avd-NFC hydrogel. According to our unpublished stability analyses, Avd-NFC hydrogel retains its biotin-binding capacity well over 1 year when stored at +4 °C or at RT. Simultaneously, it is


https://doi.org/10.1021/acs.biomac.1c00579
Biomacromolecules 2021, 22, 4122−4137

known that the avidin−biotin bond is very stable. Therefore, Avd-NFC hydrogel provides a robust platform for experiments lasting for weeks or even months.

## 4. CONCLUSIONS

We showed that conjugation of avidin on aNFC allows the use of the avidin−biotin interaction to functionalize the avidin-conjugated hydrogel (Avd-NFC) with B-FN and B-VN, providing cell adhesion motifs. The Avd-NFC hydrogel functionalized with B-FN or B-VN was successfully used in 3D cell culture experiments using MEFs. Cell adhesion studies verified that B-FN or B-VN were anchored into the hydrogel as the cells were able to produce force-dependent adhesions. We observed higher cell proliferation rates when biotinylated proteins were bound to the Avd-NFC hydrogel than that seen in cells cultured in Avd-NFC alone. As Avd-NFC hydrogel would allow functionalization virtually by any biotinylated molecule, it may find its use in various 3D cell culture applications.

## ■ ASSOCIATED CONTENT

### Supporting Information

The Supporting Information is available free of charge at https://pubs.acs.org/doi/10.1021/acs.biomac.1c00579.

Details of antibodies used in Western blot analysis; results of rheological analysis of Avd-NFC, Avd-NFC + B-FN, and Avd-NFC + B-VN; results of two parallel cell viability assays of Avd-NFC hydrogels (original data); results of cell viability assay of Avd-NFC + B-VN using different cell seeding densities; results of cell viability assay of GrowDex-A hydrogels; confocal microscopy images of Live/Dead-stained GrowDex-A samples; and Western blots used for analysis of FAK phosphorylation (PDF)

## ■ AUTHOR INFORMATION


### Corresponding Authors

**Jenni Leppiniemi** − *Faculty of Medicine and Health Technology and BioMediTech, Tampere University, FI-33014 Tampere, Finland;* orcid.org/0000-0002-7225-1648; Email: jenni.leppiniemi@tuni.fi

**Vesa P. Hytönen** − *Faculty of Medicine and Health Technology and BioMediTech, Tampere University, FI-33014 Tampere, Finland; Fimlab Laboratories, FI-33520 Tampere, Finland;* orcid.org/0000-0002-9357-1480; Email: vesa.hytonen@tuni.fi

### Authors

**Zeeshan Mutahir** − *Faculty of Medicine and Health Technology and BioMediTech, Tampere University, FI-33014 Tampere, Finland; School of Biochemistry and Biotechnology, University of the Punjab, 54590 Lahore, Pakistan*

**Alexander Dulebo** − *JPK BioAFM Business, Bruker Nano GmbH, 12489 Berlin, Germany*

**Piia Mikkonen** − *UPM-Kymmene Corporation, 00101 Helsinki, Finland*

**Markus Nuopponen** − *UPM-Kymmene Corporation, 00101 Helsinki, Finland*

**Paula Turkki** − *Faculty of Medicine and Health Technology and BioMediTech, Tampere University, FI-33014 Tampere, Finland; Fimlab Laboratories, FI-33520 Tampere, Finland*

Complete contact information is available at: https://pubs.acs.org/10.1021/acs.biomac.1c00579


### Author Contributions

Designed the study and planned the experiments: J.L., Z.M., P.M., M.N., P.T., and V.P.H. Performed the experiments: J.L., Z.M., and A.D. Analyzed the data: J.L., Z.M., and A.D. Wrote the original draft: J.L. and Z.M. Reviewed and edited the final manuscript: J.L., Z.M., A.D., P.M., M.N., P.T., and V.P.H. All authors have given approval to the final version of the manuscript.

### Notes

The authors declare no competing financial interest.

## ■ ACKNOWLEDGMENTS

This research was supported by the Academy of Finland (grants 290506 and 331946 to V.P.H.) and a grant of the Finnish Cultural Foundation to J.L. In addition, UPM Biomedicals funded part of the work of J.L. We acknowledge the Tampere Facility of Protein Services and Tampere Imaging Facility, both affiliated with the Biocenter Finland, for their services. We thank Ulla Kiiskinen, Niklas Kähkönen, and Merja Jokela (Tampere University) and the application laboratory personnel at the UPM North European Research Center for excellent technical support. We also thank MSc Latifeh Azizi for her advice on cell culture experiments and PhD Rolle Rahikainen for discussions and useful advice in setting up the 3D cell culture.

## ■ ABBREVIATIONS

2D, two-dimensional; 3D, three-dimensional; aNFC, anionic nanofibrillar cellulose; Avd, avidin; Avd-NFC, avidin-conjugated nanofibrillar cellulose; B5F, biotin-5-fluorescein; B-FN, biotinylated fibronectin; B-VN, biotinylated vitronectin; CNAvd, charge-neutralized avidin; EDC, 1-ethyl-3-(3-dimethylaminopropyl)carbodiimide hydrochloride; FBS, fetal bovine serum; HABA, 4′-hydroxyazobenzene-2-carboxylic acid; MEF, mouse embryonic fibroblast; NFC, nanofibrillar cellulose; NHS, *N*-hydroxysuccinimide; PBS, phosphate-buffered saline; RGD, tripeptide arginine-glycine-aspartate; RT, room temperature; SDS-PAGE, sodium dodecyl sulfate polyacrylamide gel electrophoresis

## ■ REFERENCES


(1) Frantz, C.; Stewart, K. M.; Weaver, V. M. The extracellular matrix at a glance. *J. Cell Sci.* **2010**, *123*, 4195.

(2) Tibbitt, M. W.; Anseth, K. S. Hydrogels as extracellular matrix mimics for 3D cell culture. *Biotechnol. Bioeng.* **2009**, *103*, 655−663.

(3) Liu, H.; Wang, Y.; Cui, K.; Guo, Y.; Zhang, X.; Qin, J. Advances in Hydrogels in Organoids and Organs-on-a-Chip. *Adv. Mater.* **2019**, *31*, 1902042.

(4) Ullah, F.; Othman, M. B. H.; Javed, F.; Ahmad, Z.; Akil, H. M. Classification, processing and application of hydrogels: A review. *Mater. Sci. Eng., C* **2015**, *57*, 414−433.

(5) Peppas, N. A.; Khare, A. R. Preparation, structure and diffusional behavior of hydrogels in controlled release. *Adv. Drug Delivery Rev.* **1993**, *11*, 1−35.

(6) Buwalda, S. J.; Boere, K. W. M.; Dijkstra, P. J.; Feijen, J.; Vermonden, T.; Hennink, W. E. Hydrogels in a historical perspective: From simple networks to smart materials. *J. Controlled Release* **2014**, *190*, 254−273.

(7) Camci-Unal, G.; Annabi, N.; Dokmeci, M. R.; Liao, R.; Khademhosseini, A. Hydrogels for cardiac tissue engineering. *NPG Asia Mater.* **2014**, *6*, No. e99.

(8) Alves, D. A.; Machado, D.; Melo, A.; Pereira, R. F.; Severino, P.; de Hollanda, L. M.; Araújo, D. R.; Lancellotti, M. Preparation of Thermosensitive Gel for Controlled Release of Levofloxacin and Their Application in the Treatment of Multidrug-Resistant Bacteria. *BioMed Res. Int.* **2016**, *2016*, 9702129.
(9) Jung, I. Y.; Kim, J. S.; Choi, B. R.; Lee, K.; Lee, H. Hydrogel Based Biosensors for In Vitro Diagnostics of Biochemicals, Proteins, and Genes. *Adv. Healthcare Mater.* **2017**, *6*, 1601475.
(10) Thiele, J.; Ma, Y.; Bruekers, S. M. C.; Ma, S.; Huck, W. T. S. 25th Anniversary Article: Designer Hydrogels for Cell Cultures: A Materials Selection Guide. *Adv. Mater.* **2014**, *26*, 125−148.
(11) Green, J. J.; Elisseeff, J. H. Mimicking biological functionality with polymers for biomedical applications. *Nature* **2016**, *540*, 386−394.
(12) Lin, N.; Dufresne, A. Nanocellulose in biomedicine: Current status and future prospect. *Eur. Polym. J.* **2014**, *59*, 302−325.
(13) Chinga-Carrasco, G.; Syverud, K. Pretreatment-dependent surface chemistry of wood nanocellulose for pH-sensitive hydrogels. *J. Biomater. Appl.* **2014**, *29*, 423−432.
(14) De France, K. J.; Hoare, T.; Cranston, E. D. Review of Hydrogels and Aerogels Containing Nanocellulose. *Chem. Mater.* **2017**, *29*, 4609−4631.
(15) Curvello, R.; Raghuwanshi, V. S.; Garnier, G. Engineering nanocellulose hydrogels for biomedical applications. *Adv. Colloid Interface Sci.* **2019**, *267*, 47−61.
(16) Dufresne, A. Nanocellulose: a new ageless bionanomaterial. *Mater. Today* **2013**, *16*, 220−227.
(17) Saito, T.; Nishiyama, Y.; Putaux, J.-L.; Vignon, M.; Isogai, A. Homogeneous Suspensions of Individualized Microfibrils from TEMPO-Catalyzed Oxidation of Native Cellulose. *Biomacromolecules* **2006**, *7*, 1687−1691.
(18) Isogai, A.; Saito, T.; Fukuzumi, H. TEMPO-oxidized cellulose nanofibers. *Nanoscale* **2011**, *3*, 71−85.
(19) Bhattacharya, M.; Malinen, M. M.; Lauren, P.; Lou, Y.-R.; Kuisma, S. W.; Kanninen, L.; Lille, M.; Corlu, A.; GuGuen-Guillouzo, C.; Ikkala, O.; Laukkanen, A.; Urtti, A.; Yliperttula, M. Nanofibrillar cellulose hydrogel promotes three-dimensional liver cell culture. *J. Controlled Release* **2012**, *164*, 291−298.
(20) Malinen, M. M.; Kanninen, L. K.; Corlu, A.; Isoniemi, H. M.; Lou, Y.-R.; Yliperttula, M. L.; Urtti, A. O. Differentiation of liver progenitor cell line to functional organotypic cultures in 3D nanofibrillar cellulose and hyaluronan-gelatin hydrogels. *Biomaterials* **2014**, *35*, 5110−5121.
(21) Lou, Y.-R.; Kanninen, L.; Kuisma, T.; Niklander, J.; Noon, L. A.; Burks, D.; Urtti, A.; Yliperttula, M. The use of nanofibrillar cellulose hydrogel as a flexible three-dimensional model to culture human pluripotent stem cells. *Stem Cells Dev.* **2014**, *23*, 380−392.
(22) Laurén, P.; Somersalo, P.; Pitkänen, I.; Lou, Y.; Urtti, A.; Partanen, J.; Seppälä, J.; Madetoja, M.; Laaksonen, T.; Mäkitie, A.; Yliperttula, M. Nanofibrillar cellulose-alginate hydrogel coated surgical sutures as cell-carrier systems. *PLoS One* **2017**, *12*, No. e0183487.
(23) Azoidis, I.; Metcalfe, J.; Reynolds, J.; Keeton, S.; Hakki, S. S.; Sheard, J.; Widera, D. Three-dimensional cell culture of human mesenchymal stem cells in nanofibrillar cellulose hydrogels. *MRS Commun.* **2017**, *7*, 458−465.
(24) Xu, W.; Wang, X.; Sandler, N.; Willför, S.; Xu, C. Three-Dimensional Printing of Wood-Derived Biopolymers: A Review Focused on Biomedical Applications. *ACS Sustainable Chem. Eng.* **2018**, *6*, 5663−5680.
(25) Sheard, J. J.; Bicer, M.; Meng, Y.; Frigo, A.; Aguilar, R. M.; Vallance, T. M.; Iandolo, D.; Widera, D. Optically Transparent Anionic Nanofibrillar Cellulose Is Cytocompatible with Human Adipose Tissue-Derived Stem Cells and Allows Simple Imaging in 3D. *Stem Cells Int.* **2019**, *2019*, 3106929.
(26) Chang, H.-T.; Heuer, R. A.; Oleksijew, A. M.; Coots, K. S.; Roque, C. B.; Nella, K. T.; McGuire, T. L.; Matsuoka, A. J. An engineered three-dimensional stem cell niche in the inner ear by applying a nanofibrillar cellulose hydrogel with a sustained-release neurotrophic factor delivery system. *Acta Biomater.* **2020**, *108*, 111−127.
(27) Foyt, D. A.; Norman, M. D. A.; Yu, T. T. L.; Gentleman, E. Exploiting Advanced Hydrogel Technologies to Address Key Challenges in Regenerative Medicine. *Adv. Healthcare Mater.* **2018**, *7*, 1700939.
(28) Hern, D. L.; Hubbell, J. A. Incorporation of adhesion peptides into nonadhesive hydrogels useful for tissue resurfacing. *J. Biomed. Mater. Res.* **1998**, *39*, 266−276.
(29) Lutolf, M. P.; Lauer-Fields, J. L.; Schmoekel, H. G.; Metters, A. T.; Weber, F. E.; Fields, G. B.; Hubbell, J. A. Synthetic matrix metalloproteinase-sensitive hydrogels for the conduction of tissue regeneration: Engineering cell-invasion characteristics. *Proc. Natl. Acad. Sci. U.S.A.* **2003**, *100*, 5413−5418.
(30) Barros, D.; Conde-Sousa, E.; Gonçalves, A. M.; Han, W. M.; García, A. J.; Amaral, I. F.; Pêgo, A. P. Engineering hydrogels with affinity-bound laminin as 3D neural stem cell culture systems. *Biomater. Sci.* **2019**, *7*, 5338−5349.
(31) Hytönen, V. P.; Määttä, J. A. E.; Nyholm, T. K. M.; Livnah, O.; Eisenberg-Domovich, Y.; Hyre, D.; Nordlund, H. R.; Hörhä, J.; Niskanen, E. A.; Paldanius, T.; Kulomaa, T.; Porkka, E. J.; Stayton, P. S.; Laitinen, O. H.; Kulomaa, M. S. Design and construction of highly stable, protease-resistant chimeric avidins. *J. Biol. Chem.* **2005**, *280*, 10228−10233.
(32) Rosano, C.; Arosio, P.; Bolognesi, M. The X-ray three-dimensional structure of avidin. *Biomol. Eng.* **1999**, *16*, 5−12.
(33) Laitinen, O. H.; Nordlund, H. R.; Hytönen, V. P.; Kulomaa, M. S. Brave new (strept)avidins in biotechnology. *Trends Biotechnol.* **2007**, *25*, 269−277.
(34) Tsai, W.-B.; Wang, P.-Y.; Chang, Y.; Wang, M.-C. Fibronectin and culture temperature modulate the efficacy of an avidin-biotin binding system for chondrocyte adhesion and growth on biodegradable polymers. *Biotechnol. Bioeng.* **2007**, *98*, 498−507.
(35) Kämmerer, P. W.; Lehnert, M.; Al-Nawas, B.; Kumar, V. V.; Hagmann, S.; Alshihri, A.; Frerich, B.; Veith, M. Osseoconductivity of a Specific Streptavidin-Biotin-Fibronectin Surface Coating of Biotinylated Titanium Implants - A Rabbit Animal Study. *Clin. Implant Dent. Relat. Res.* **2015**, *17*, No. e601.
(36) Leppiniemi, J.; Lahtinen, P.; Paajanen, A.; Mahlberg, R.; Metsä-Kortelainen, S.; Pinomaa, T.; Pajari, H.; Vikholm-Lundin, I.; Pursula, P.; Hytönen, V. P. 3D-Printable Bioactivated Nanocellulose-Alginate Hydrogels. *ACS Appl. Mater. Interfaces* **2017**, *9*, 21959−21970.
(37) Gering, C.; Koivisto, J. T.; Parraga, J.; Leppiniemi, J.; Vuornos, K.; Hytönen, V. P.; Miettinen, S.; Kellomäki, M. Design of modular gellan gum hydrogel functionalized with avidin and biotinylated adhesive ligands for cell culture applications. *PLoS One* **2019**, *14*, No. e0221931.
(38) Fernandes, C. S. M.; Rodrigues, A. L.; Alves, V. D.; Fernandes, T. G.; Pina, A. S.; Roque, A. C. A. Natural Multimerization Rules the Performance of Affinity-Based Physical Hydrogels for Stem Cell Encapsulation and Differentiation. *Biomacromolecules* **2020**, *21*, 3081−3091.
(39) Hughes, C. S.; Postovit, L. M.; Lajoie, G. A. Matrigel: a complex protein mixture required for optimal growth of cell culture. *Proteomics* **2010**, *10*, 1886−1890.
(40) Tsuchiya, H.; Sakata, N.; Yoshimatsu, G.; Fukase, M.; Aoki, T.; Ishida, M.; Katayose, Y.; Egawa, S.; Unno, M. Extracellular Matrix and Growth Factors Improve the Efficacy of Intramuscular Islet Transplantation. *PLoS One* **2015**, *10*, No. e0140910.
(41) Ray, S.; Steven, R. T.; Green, F. M.; Höök, F.; Taskinen, B.; Hytönen, V. P.; Shard, A. G. Neutralized Chimeric Avidin Binding at a Reference Biosensor Surface. *Langmuir* **2015**, *31*, 1921−1930.
(42) Ebner, A.; Marek, M.; Kaiser, K.; Kada, G.; Hahn, C. D.; Lackner, B.; Gruber, H. J. Application of biotin-4-fluorescein in homogeneous fluorescence assays for avidin, streptavidin, and biotin or biotin derivatives. *Methods Mol. Biol.* **2008**, *418*, 73−88.
(43) Yatohgo, T.; Izumi, M.; Kashiwagi, H.; Hayashi, M. Novel purification of vitronectin from human plasma by heparin affinity chromatography. *Cell Struct. Funct.* **1988**, *13*, 281−292.


https://doi.org/10.1021/acs.biomac.1c00579
*Biomacromolecules* 2021, 22, 4122−4137

(44) Green, N. M. A Spectrophotometric Assay for Avidin and Biotin Based on Binding of Dyes by Avidin. *Biochem. J.* **1965**, *94*, 23C−24C.
(45) Xu, W.; Baribault, H.; Adamson, E. D. Vinculin knockout results in heart and brain defects during embryonic development. *Development* **1998**, *125*, 327−337.
(46) Määttä, J. A. E.; Eisenberg-Domovich, Y.; Nordlund, H. R.; Hayouka, R.; Kulomaa, M. S.; Livnah, O.; Hytönen, V. P. Chimeric avidin shows stability against harsh chemical conditions-biochemical analysis and 3D structure. *Biotechnol. Bioeng.* **2011**, *108*, 481−490.
(47) Gruber, H. J.; Kada, G.; Marek, M.; Kaiser, K. Accurate titration of avidin and streptavidin with biotin-fluorophore conjugates in complex, colored biofluids. *Biochim. Biophys. Acta* **1998**, *1381*, 203−212.
(48) Oberbichler, E.; Wiesauer, M.; Schlögl, E.; Stangl, J.; Faschinger, F.; Knör, G.; Gruber, H. J.; Hytönen, V. P. Competitive binding assay for biotin and biotin derivatives, based on avidin and biotin-4-fluorescein. *Methods Enzymol.* **2020**, *633*, 1−20.
(49) Hytönen, V. P.; Laitinen, O. H.; Airenne, T. T.; Kidron, H.; Meltola, N. J.; Porkka, E. J.; Hörhä, J.; Paldanius, T.; Määttä, J. A. E.; Nordlund, H. R.; Johnson, M. S.; Salminen, T. A.; Airenne, K. J.; Yläherttuala, S.; Kulomaa, M. S. Efficient production of active chicken avidin using a bacterial signal peptide in Escherichia coli. *Biochem. J.* **2004**, *384*, 385−390.
(50) Kada, G.; Falk, H.; Gruber, H. J. Accurate measurement of avidin and streptavidin in crude biofluids with a new, optimized biotin-fluorescein conjugate. *Biochim. Biophys. Acta* **1999**, *1427*, 33−43.
(51) Ke, S.; Wright, J. C.; Kwon, G. S. Intermolecular Interaction of Avidin and PEGylated Biotin. *Bioconjugate Chem.* **2007**, *18*, 2109−2114.
(52) Livnah, O.; Bayer, E. A.; Wilchek, M.; Sussman, J. L. Three-dimensional structures of avidin and the avidin-biotin complex. *Proc. Natl. Acad. Sci. U.S.A.* **1993**, *90*, 5076−5080.
(53) Shao, D.; Tapio, K.; Auer, S.; Toppari, J. J.; Hytönen, V. P.; Ahlskog, M. Surface Characteristics Control the Attachment and Functionality of (Chimeric) Avidin. *Langmuir* **2018**, *34*, 15335−15342.
(54) Bachmann, M.; Schäfer, M.; Mykuliak, V. V.; Ripamonti, M.; Heiser, L.; Weißenbruch, K.; Krübel, S.; Franz, C. M.; Hytönen, V. P.; Wehrle-Haller, B.; Bastmeyer, M. Induction of ligand promiscuity of $\alpha V\beta 3$ integrin by mechanical force. *J. Cell Sci.* **2020**, *133*, jcs242404.
(55) Smithmyer, M. E.; Sawicki, L. A.; Kloxin, A. M. Hydrogel scaffolds asin vitromodels to study fibroblast activation in wound healing and disease. *Biomater. Sci.* **2014**, *2*, 634−650.
(56) Bott, K.; Upton, Z.; Schrobback, K.; Ehrbar, M.; Hubbell, J. A.; Lutolf, M. P.; Rizzi, S. C. The effect of matrix characteristics on fibroblast proliferation in 3D gels. *Biomaterials* **2010**, *31*, 8454−8464.
(57) Pankov, R.; Yamada, K. M. Fibronectin at a glance. *J. Cell Sci.* **2002**, *115*, 3861−3863.
(58) Preissner, K. T.; Seiffert, D. Role of Vitronectin and Its Receptors in Haemostasis and Vascular Remodeling. *Thromb. Res.* **1998**, *89*, 1−21.
(59) Wierzbicka-Patynowski, I.; Schwarzbauer, J. E. The ins and outs of fibronectin matrix assembly. *J. Cell Sci.* **2003**, *116*, 3269−3276.
(60) Broguiere, N.; Isenmann, L.; Hirt, C.; Ringel, T.; Placzek, S.; Cavalli, E.; Ringnalda, F.; Villiger, L.; Züllig, R.; Lehmann, R.; Rogler, G.; Heim, M. H.; Schüler, J.; Zenobi-Wong, M.; Schwank, G. Growth of Epithelial Organoids in a Defined Hydrogel. *Adv. Mater.* **2018**, *30*, No. e1801621.
(61) Enemchukwu, N. O.; Cruz-Acuña, R.; Bongiorno, T.; Johnson, C. T.; García, J. R.; Sulchek, T.; García, A. J. Synthetic matrices reveal contributions of ECM biophysical and biochemical properties to epithelial morphogenesis. *J. Cell Biol.* **2016**, *212*, 113−124.
(62) Curvello, R.; Kerr, G.; Micati, D. J.; Chan, W. H.; Raghuwanshi, V. S.; Rosenbluh, J.; Abud, H. E.; Garnier, G. Engineered Plant-Based Nanocellulose Hydrogel for Small Intestinal Organoid Growth. *Adv. Sci.* **2021**, *8*, 2002135.
(63) Wacker, B. K.; Alford, S. K.; Scott, E. A.; Das Thakur, M.; Longmore, G. D.; Elbert, D. L. Endothelial Cell Migration on RGD-Peptide-Containing PEG Hydrogels in the Presence of Sphingosine 1-Phosphate. *Biophys. J.* **2008**, *94*, 273−285.
(64) Kumagai, H.; Tajima, M.; Ueno, Y.; Giga-Hama, Y.; Ohba, M. Effect of cyclic RGD peptide on cell adhesion and tumor metastasis. *Biochem. Biophys. Res. Commun.* **1991**, *177*, 74−82.
(65) Kapp, T. G.; Rechenmacher, F.; Neubauer, S.; Maltsev, O. V.; Cavalcanti-Adam, E. A.; Zarka, R.; Reuning, U.; Notni, J.; Wester, H.-J.; Mas-Moruno, C.; Spatz, J.; Geiger, B.; Kessler, H. A Comprehensive Evaluation of the Activity and Selectivity Profile of Ligands for RGD-binding Integrins. *Sci. Rep.* **2017**, *7*, 39805.
(66) Arnaout, M. A.; Goodman, S. L.; Xiong, J.-P. Structure and mechanics of integrin-based cell adhesion. *Curr. Opin. Cell Biol.* **2007**, *19*, 495−507.
(67) Campbell, I. D.; Humphries, M. J. Integrin structure, activation, and interactions. *Cold Spring Harbor Perspect. Biol.* **2011**, *3*, a004994.
(68) Blondel, D.; Lutolf, M. P. Bioinspired Hydrogels for 3D Organoid Culture. *Chimia* **2019**, *73*, 81−85.
(69) Bayer, E. A.; Wilchek, M. [14] Protein biotinylation. *Methods Enzymol.* **1990**, *184*, 138−160.
(70) Beckett, D.; Kovaleva, E.; Schatz, P. J. A minimal peptide substrate in biotin holoenzyme synthetase-catalyzed biotinylation. *Protein Sci.* **1999**, *8*, 921−929.
(71) Fairhead, M.; Howarth, M. Site-specific biotinylation of purified proteins using BirA. *Methods Mol. Biol.* **2015**, *1266*, 171−184.


https://doi.org/10.1021/acs.biomac.1c00579
*Biomacromolecules* 2021, 22, 4122−4137